BOREAL ENVIRONMENT RESEARCH 19 (suppl. A): 4–30
ISSN 1239-6095 (print) ISSN 1797-2469 (online)
© 2014
Helsinki 21 March 2014

Climate variability and trends in the Valkea-Kotinen region, southern Finland: comparisons between the past, current and projected climates

Kirsti Jylhä[1)], Mikko Laapas[1)], Kimmo Ruosteenoja[1)], Lauri Arvola[2)], Achim Drebs[1)], Juha Kersalo[1)], Seppo Saku[1)], Hilppa Gregow[1)], Henna-Reetta Hannula[1)] and Pentti Pirinen[1)]

[1)] *Finnish Meteorological Institute, P.O. Box 506, FI-00101 Helsinki, Finland*
[2)] *University of Helsinki, Lammi Biological Station, Pääjärventie 320, FI-16900 Lammi, Finland*

Received 22 Mar. 2013, final version received 11 Oct. 2013, accepted 3 Oct. 2013

Jylhä, K., Laapas, M., Ruosteenoja, K., Arvola, L., Drebs, A., Kersalo, J., Saku, S., Gregow, H., Hannula, H.-R. & Pirinen, P. 2014: Climate variability and trends in the Valkea-Kotinen region, southern Finland: comparisons between the past, current and projected climates. *Boreal Env. Res.* 19 (suppl. A): 4–30.

Climate variability and temporal trends in the period 1990–2010 around the Valkea-Kotinen environmental monitoring area were compared both with earlier observations and with climate model projections for the 2040s and 2080s. The focus was on climatic variables relevant for aquatic and terrestrial ecosystems, i.e., air temperature, precipitation, snow depth, lake-ice cover, wind speed and solar radiation. Changes in these variables were categorized depending on how rapidly they are likely to emerge from the background of recently-experienced inter-annual variability. The statistically significant increases in annual and spring mean temperatures of about 0.4 °C per decade, observed during the period 1964–2011, are projected to continue in the future, accompanied by corresponding changes in snow depth and lake-ice duration. Based on the multi-model mean estimates, increases in annual mean precipitation and decreases in winter solar radiation would become statistically significant by the 2040s. In addition to the recorded inter-annual variability, inter-model uncertainty intervals were considered.

Introduction

Air temperature, precipitation and other meteorological variables affect ecosystems at various temporal scales. Climate, described by the averages and typical year-to-year fluctuations of weather, is one of the key factors that control processes in ecosystems and habitat ranges of species on a time scale of years to decades. In a shorter term, extreme weather and climate events, like heat waves or strong winds, may disturb ecosystems and affect species diversity. Climatic information on decadal and centennial scales is also needed to understand ecosystem performance, as the health or productivity of an ecosystem component may be exposed to natural or human-induced changes in climate (Forsius *et al*. 2013 and references therein).

The Valkea-Kotinen environmental monitoring area, comprising altogether 30 hectares of forests, bogs and waterbodies (1 in Fig. 1), is located in southern Finland in the Kotinen nature reserve area (61°14´N, 25°04´E). According to a globally-used climate classification system

Editor in charge of this article: Veli-Matti Kerminen

(Köppen 1936), the region belongs to the boreal subzone Dfc (Jylhä *et al*. 2010). This zone is characterized by cold and snowy winters, with the coolest month having a mean temperature below –3 °C, moderate precipitation in all seasons, and relatively short and cool summers, with at most three months having a mean temperature above 10 °C (e.g., Critchfield 1966, Jylhä *et al*. 2010). In the Finnish bioclimatic zone system (Ahti *et al*. 1968), the site is located in the southern boreal zone (Solantie 2005, Hällfors *et al*. 2011). In a third classification, the Finnish growing zone scheme for horticulture, the area is close to the border between the second and third zones on a scale of eight in which 8 represents the least favourable area from the point of view of plant survival (Solantie 2004); this classification is based the effective temperature sum, the length of the growing season, and the mean of the three lowest recorded temperatures during a period of three decades (Solantie 1986, 1988). Finally, if the country is divided into five main snow regions to the south of the Arctic Circle, Valkea-Kotinen is situated in a transition sector between the regions two and three in an ascending order of snowiness (Solantie 2000).

Ecosystem monitoring was started in the Valkea-Kotinen region in 1987 (Vuorenmaa *et al*. 2011). Before that, meteorological conditions had been systematically measured for almost a quarter of century at the Lammi Pappila weather station, situated on the premises the Lammi Biological Station about 20 km to the south (station 4 in Fig. 1). Within a distance of less than 50 km of Valkea-Kotinen, an even longer time series of climate data are available from the weather station at Hattula Lepaa (6 in Fig. 1). That station was founded in 1926 to supplement the Finnish weather station network which was set up in the late 19th century and achieved its peak number of sites in the 1970s (Tietäväinen *et al*. 2010).

Observations from a time-evolving network of weather stations can be spatially interpolated to constitute gridded climate data sets. These are used, for example, as surrogate information at locations that lack observations in place or time. A widely-used gridded data set for climate in Europe since the 1950s was generated by Haylock *et al*. (2008) and this data set has been regularly updated thereafter. Gridded data covering

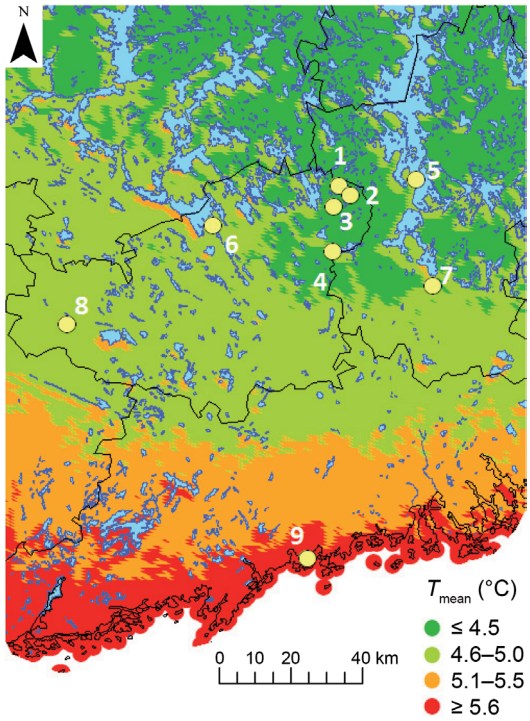

Fig. 1. The annual mean temperature (°C) in southern Finland in 1990–2010. Light blue areas are lakes, and the black contours show provincial boundaries. The observation stations numbered 1 to 9 are detailed in Table 1. The temperature data are adopted from Aalto *et al.* (2013).

Finland have been available since the year 1847 for monthly mean temperature (Tietäväinen *et al*. 2010), since 1908 for the May–September monthly precipitation sum (Ylhäisi *et al*. 2010), since 1919 for snow depth on 15 March (Solantie 2000, Hannula 2012) and since 1947 for snow depth on 15 January (Solantie 2000). Since 1961, these data sets have been accompanied by daily (Venäläinen *et al*. 2005) and monthly (Aalto *et al*. 2013) gridded climate data sets at spatial resolutions of 10 km and 1 km, respectively.

Statistics based on meteorological observations depict past climate only. Possible trends in these observations cannot be extrapolated into the future, because the global climate system is responding to on-going changes in atmospheric concentrations of greenhouse gases (GHGs) and aerosols. Based on the data provided by NOAA (http://www.esrl.noaa.gov/gmd/ccgg/trends/), the global CO_2 content increased by almost 5%

per decade during the period 1990–2010, reducing the thermal radiation flux into space. Concurrently, an opposing phenomenon related to aerosols started to decline. Solar radiation measured at the Earth's surface was found to weaken in Europe from the 1950s to the 1980s, and this "dimming" was mainly attributed to growing aerosol precursor emissions at that time (Wild and Schmucki 2011). Since then, the aerosol loading has decreased in Europe, as evidenced by the rapidly-declining trends of SO_4^{2-} in the air and in the deposition at the Finnish air quality background stations (Ruoho-Airola 2012, Ruoho-Airola *et al*. 2014). In the future, atmospheric concentrations of GHGs and aerosols will continue to change, the exact rate depending on the temporal evolution of the emissions (*see* e.g., Taylor *et al*. 2012).

In order to assess how the anthropogenic climate change and its environmental impacts will materialize in the Valkea-Kotinen region in the future, climate scenarios are needed. These are based on simulations performed with global climate models (GCMs). The spatial resolution of the output data from GCMs is generally rather modest, but it can be improved by dynamical regionalization (Rummukainen 2010) or by empirical/statistical downscaling (Willems *et al*. 2012). For climatic variables for which changes are regionally fairly smooth, like those to be considered here, a simpler alternative is to bi-linearly interpolate coarse resolution model projections onto a finer-scale landscape map, optionally differentiating between land and sea grid points, or between high- and lowlands. Various procedures are then available for minimizing the influence of biases that exist in model descriptions of the present-day climate (Graham *et al*. 2007, Räisänen and Räty 2013).

In this paper, climatic conditions in the Valkea-Kotinen region during 1990–2010 are compared with the preceding climate based on observations and with the projected future climate based on climate model simulations. The focus is on describing variations and potential trends in climatic variables relevant for aquatic and terrestrial ecosystems, i.e., air temperature, precipitation, snow depth, lake ice cover, wind speed and solar radiation. The incorporation of both climate observations and scenarios allows us to see the modelled future changes in the perspective of already-observed trends and also to use the range of recently-observed temporal variability to assess the significance of the modelled trends. Our goal is to address the question of how rapidly climate will change in the future as compared with what the ecosystems in the Valkea-Kotinen region have recently experienced.

Material and methods

Observational data

Three main types of Finnish Meteorological Institute (FMI) observational weather data sets were used here to examine climate conditions in the surroundings of the Valkea-Kotinen environmental monitoring area. These included (1) daily measurements of air temperature, precipitation, snow depth, wind speed, and incident solar radiation at nearby synoptic weather stations; (2) gridded monthly mean temperature and precipitation data; and (3) gridded data of snow depth values on 15 March.

The weather stations considered here are numbered 2–8 (Fig. 1). Number 1 marks the Kotinen air quality monitoring site; number 9 shows the position of the oldest weather station still operating in Finland (Kaisaniemi in Helsinki), at a distance of about 120 km to the south of Valkea-Kotinen. Neither of the weather stations closest to the Valkea-Kotinen catchment, numbered 2 and 3, provides data for the whole period 1990–2010 (Table 1). We therefore selected station 4 (Lammi Pappila) that has operated for about 50 years as a reference weather station for temperature, precipitation and snow depth. It is located 21 km to the south of station 1 at an elevation of 125 m a.m.s.l. (i.e. 33 m lower than station 1). As will be shown later, station 4 illustrates climate in the Valkea-Kotinen area moderately well.

Since measurements of temperature and precipitation are lacking from station 4 prior to 1964, gridded monthly mean data at a 10-km spatial resolution served as surrogates. The data sets were produced by Tietäväinen *et al*. (2010) and Ylhäisi e*t al*. (2010) using the krig-

ing method. This method interpolates grid-point values from actual measurements primarily based on spatial autocorrelations. It also utilizes information on elevation and the sea and lake fractions (for details, *see* Aalto *et al*. 2013).

For snow depth, reference measurements from station 4 were also supplemented with gridded information. Snow depth on 15 March has been measured, mostly by volunteers, all over the country since 1919. The data were analysed on a 20 × 20 km^2 grid by Solantie (2000). The number of voluntary observations has declined from year to year, which poses a risk to the reliability of the gridded data.

This study additionally utilizes observations made at stations 5–8 (Fig. 1 and Table 1). In order to address extreme weather events, long time series are preferred, because the reliability of the analysis largely depends on the length and quality of the time series (e.g., Venäläinen *et al*. 2007, 2009). According to Saku *et al*. (2011), very high temperatures, with a recurrence period of 20–50 years or longer, have geographically a rather uniform distribution in Finland. We therefore decided to use the data from station 6 (Hattula Lepaa) for daily maximum temperature. That station has the longest time series of weather data within 50 km of Valkea-Kotinen, as it was launched in the 1920s and has been slightly relocated only once in 2008.

In the absence of on-going wind measurements at stations 3–4 and 6, and due to the short time series at station 2, we incorporated stations 5 (Asikkala), 7 (Lahti Laune) and 8 (Jokioinen) into the research material. Ten-minute average wind speeds, mostly at three-hour intervals, have been measured at these stations for 20–55 years (Table 1). To describe wind conditions in Finland in 1981–2010, of these stations Pirinen *et al*. (2012) only accepted station 8, since this has the longest and most reliable time series for wind. We also examined the probability of occurrence of high wind speeds using station 8 alone. At that station incident solar radiation and the state of precipitation (liquid, solid or a mixture) were also recorded.

In addition to the meteorological data from FMI, we used observations, conducted by the Lammi Biological Station, University of Helsinki, of seasonal ice on the Lake Valkea-Kotinen

Table 1. Observation stations (numbered as in Fig. 1). The identifier refers to the WMO index number (or a national identification number in parentheses). Variables: T_{mean} and T_{max} are the mean and daily maximum temperatures, respectively; P and P_F are the precipitation sum and form, respectively; S is the snow depth; W is the wind speed; R is the solar radiation.

No.	Name	Identifier	Lat. (°N)	Long. (°E)	Altitude (m a.m.s.l.)	Distance to station 1 (km)	Station in operation	Variables used in the study
1	Valkea-Kotinen	(1437)	61.24	25.07	158	0	since 1 Apr. 1987	–
2	Lammi Evo	02713	61.22	25.13	134	4.5	since 1 Nov. 2005	T_{mean}, W
3	Lammi Iso-Evo	02783	61.18	25.04	129	6.5	15 Sep. 1988–1 Feb. 2009	T_{mean}, P
4	Lammi Pappila	02767	61.05	25.04	125	20.8	since 1 July 1963	T_{mean}, P, S
5	Asikkala	02727	61.27	25.52	80	24.6	since 7 June 1991	W
6	Hattula Lepaa*	02704	61.11	24.32	87	42.2	since 1 July 1926	T_{max}
7	Lahti Laune	02965	60.96	25.63	78	43.5	since 1 Jan. 1961	W
8	Jokioinen	02963	60.81	23.50	104	97.1	since 1 Jan. 1957	W, R, P_F
9	Helsinki	02978	60.18	24.94	4	118.8	since 1 July 1844	–

* The station was slightly relocated in 2008; the previous WMO index number was 05184.

since 1990. Three lake ice parameters have been recorded: ice-on and ice-off (i.e. ice break-up) dates and the length (number of days) of the ice season. The ice-on date was defined as the day when the lake was completely frozen and did not melt until the following spring. The ice break-up was defined to occur when > 50% of the lake area was free of ice.

Analysis of the observations

Following the guidance of the World Meteorological Organization (WMO), averages of climatological data are commonly computed for periods of three decades (WMO 2011). A 30-year period is preferred, as it is long enough to filter out any inter-annual variation or anomalies, with no individual year being given too much weight. Nonetheless, in the current study on the climate in the Valkea-Kotinen region, we used a 21-year period 1990–2010 as a reference. Longer partly-overlapping or preceding time intervals were also considered for comparison.

Seasonal means were computed as three-month averages centred in January, April, July and October. Based on visual inspections, the probability distributions of the variables varied in shape from season to season, and depending on the degree of time averaging.

Statistical significance of temperature differences at station 4 between the reference period 1990–2010 and the preceding period 1964–1989 was examined using a two-sample Welch *t*-test (Wt) that assumes the variables to have a probability distribution close to Gaussian. For the other variables, we applied a non-parametric Mann-Whitney (MW) test (also called Mann-Whitney-Wilcoxon rank-sum test; Wilks 2006) instead. Differences between the stations during their common operational times were studied using the same two tests in order to explore how suitable station 4 (station 8 in the case of wind) was for describing the mean climatological conditions in the Valkea-Kotinen region. The R Stats Package within R (R Core Team 2012) was used.

The trends were primarily studied using a non-parametric Mann-Kendall (MK) test for a monotonic trend and the Theil-Sen estimate of the slope (Helsel and Hirsch 2002).

In order to utilize all monthly data to assess trends in annual means, we additionally applied two methods. The first alternative comprised of seasonal Mann-Kendall trend testing (Hirsch *et al*. 1982, Marchetto *et al*. 2013), provided by the R *rkt* package (http://cran.r-project.org/web/packages/rkt/rkt.pdf). The second procedure applied the ITSM 2000 software package (ver. 7.3), developed by Brockwell and Davis (2002). We first removed seasonal components and then applied a generalized least-squares linear regression. If we found a statistically-significant trend, we examined the generated sequence of residuals and aimed to find an appropriate autoregressive moving average (ARMA) model for them. Lastly, the standard error of the trend line slope was reassessed to obtain a final estimate of the significance level of the trend. For further details, *see* Ruoho-Airola *et al*. (2014).

The occurrence of days with air temperature above (or below) certain thresholds were examined as examples of temperature indices. Furthermore, probabilities of the occurrence of unusually high values of instantaneous air temperature at station 6 and ten-minute average wind speeds at station 8 were estimated by fitting a generalized extreme value (GEV) distribution to the recorded annual maxima. For wind speed, the maxima of each calendar month were additionally examined. For temperature, an alternative approach called the "peaks over threshold" (POT) method was also used for the sake of comparison. That technique considers the generalized Pareto distribution (GPD) and exploits not only annual maxima but other high data values as well. Both distributions are characterized by shape, location and scale parameters (Coles 2001). Since the time series of the maxima, almost without exception, did not suggest any statistically significant trends or heteroscedasticity, we regarded these three parameters constant in time. They were estimated objectively with the method of maximum likelihood (Coles 2001) and then used to calculate the return levels corresponding to various return periods. The 95% confidence intervals of the return levels were based on the profile likelihood method (Coles 2001). The packages *ismev*, *evd* and *extRemes* in R were used.

Climate model data and scenarios

We utilized the monthly mean output data from 19 coupled atmosphere–ocean GCMs in order to project changes in temperature and precipitation in the Valkea-Kotinen region (Table 2). Because of missing or inadequate-quality data, projections for snow water equivalent and incident solar radiation were derived from 17–18 models and those for near-surface wind speed from 9 models. The model data were taken from the World Climate Research Programme's (WCRP's) Coupled Model Intercomparison Project phase 3 (CMIP3) multi-model dataset (Meehl *et al*. 2007). Four of the 23 models in the CMIP3 archive were abandoned because of their poor land-sea distribution or too unrealistically simulated present-day climate in northern Europe (Jylhä *et al*. 2010). Prior to further analysis, all model data were interpolated onto a common grid.

An important source of uncertainty involved in climate projections arises from unknown future emissions (and the associated concentrations and radiative forcing effects) of GHGs and aerosols into the atmosphere. The CMIP3 GCMs were run under the Intergovernmental Panel on Climate Change (IPCC) Special Report on Emissions Scenarios (SRES) A1B, A2 and B1 (Nakićenović and Swart 2000). In general, we composed the multi-model mean estimates of climatic changes separately for each emis-

Table 2. Global climate models employed in this study and availability of the data for each climate variable. *See* footnotes for further details about simulated time spans and surrogate scenario data created by pattern scaling. For more information on the models, *see* table 8.1 in IPCC (2007) and references therein.

Model	Spatial resolution (°) of the model output		Mean temp.	Precipitation	Snow water	Wind speed**	Solar radiation
	zonal direction (Δx)	meridional direction (Δy)					
BCCR-BCM2.0	1.9	1.9	x	x	x	x	x
CGCM3.1(T47)	2.8	2.8	x	x	x	–	x
CGCM3.1(T63)*	1.9	1.9	x	x	x	x	x
CNRM-CM3	1.9	1.9	x	x	x	x	x
CSIRO-MK3.0	1.9	1.9	x	x	x	x	-
ECHAM5/MPI-OM	1.9	1.9	x	x	x	x	x
ECHO-G	3.9	3.9	x	x	x	–	x
GFDL-CM2.0	2.0	2.5	x	x	x	–	x
GFDL-CM2.1	2.0	2.5	x	x	x	x	x
GISS-ER	4.0	5.0	x	x	–	–	x
INM-CM3.0	4.0	5.0	x	x	x	–	x
IPSL-CM4	2.5	3.75	x	x	x	x	x
MIROC3.2(HIRES)*	1.1	1.1	x	x	x	x	x
MIROC3.2(MEDRES)	2.8	2.8	x	x	x	–	x
MRI-CGCM2.3.2	2.8	2.8	x	x	x	x	x
NCAR-CCSM3	1.4	1.4	x	x	x	–	x
NCAR-PCM	2.8	2.8	x	x	–	–	x
UKMO-HadCM3	2.5	3.75	x	x	x	–	x
UKMO-HadGEM1	1.3	1.9	x	x	x	–	x
Number of models			19	19	17	9	18

* Model experiments under the SRES A2 are not available. In order to make the multi-model mean responses in mean temperature, precipitation, snow water and solar radiation comparable for all three GHG scenarios, surrogate data for the missing A2 runs were created by employing the pattern-scaling technique detailed in Ruosteenoja *et al.* (2007).

** Data for zonal and meridional daily wind components were available under the SRES A1B scenario alone and for the periods 1971–2000, 2046–2065 and 2081–2100 only. In order to assess the changes in climatological means for the periods 2030–2059 (around the 2040s) and 2070–2099 (around the 2080s) relative to 1990–2010, linear interpolation was used.

sion scenario. However, to obtain best estimates of the changes during the next few decades, we combined model outputs under all three emission scenarios, regarding them equally likely. This procedure is supported by the fact that during a short time horizon, the three GHG concentrations scenarios do not diverge substantially.

The climate change scenarios were given in absolute terms for mean temperature and in percentages for the other variables. The scenarios were calculated relative to the modelled 1990–2010 baseline period. Since the spatial distributions of the changes were relatively uniform, with only slightly larger increases in temperature and precipitation in northern than in southern Finland (Jylhä *et al*. 2009), we simply employed data at the closest grid point.

In the final step, we applied the delta-change method (Graham *et al*. 2007) to calculate the future climatological means. The method has the advantage of reducing the influence of model biases in representing the present-day climate. The projected increases of monthly mean temperatures were added to the recorded 21-year average monthly means in 1990–2010. For the other variables, we multiplied the calculated baseline period climatological means by the ratios of the simulated values for the future period to those for the baseline period. Percentage changes in snow depth were assumed to approximately match percentage changes in snow water equivalent.

Metrics for uncertainty and significance

Three metrics are used in the following analysis to depict and interpret the projected changes in climate. The measures are linked to the two questions: (1) Taking into account the fact that different models give different results, what are the lower and upper estimates for changes in climate? (2) How rapidly will the modelled changes become statistically significant compared with the range of inter-annual variability recently recorded at a site of interest?

For the first measure, we studied the uncertainty in the projections arising from scatter among different model simulations. Following Ruosteenoja *et al*. (2007, 2011), we fitted normal distributions to the ensembles of climate change projections calculated by the 19 climate models. For the 30-year period 2070–2099, centred on the 2080s, the normal distributions were considered separately for each GHG scenario. For the period 2020–2059, centred on the 2040s, the normal distributions for the three GHG scenarios were very alike; therefore the three distributions were linearly combined, using equal weights. The range between the 5th and 95th quantiles, denoted here by $\Delta_{90(\mathrm{model})}$, gives us lower and upper estimates for the changes. Ideally, the probability of changes larger than the upper end of $\Delta_{90(\mathrm{model})}$ is 5%, and the same is true for changes smaller than the lower end of the range. In reality, the uncertainty interval is only approximate, since the models constitute a fairly small sample and are not entirely independent of one another.

In addition to scatter among different models, the significance of projected changes is often assessed based on modelled inter-annual or inter-decadal variability (e.g., Orlowsky and Seneviratne 2012, Deser *et al*. 2012). Here, however, the purpose is to explore the statistical significance of differences between the recorded present-day and the projected future climatological means. Therefore, we tested the multi-model mean change against the observed inter-annual standard deviation, σ, derived from recorded data during a recent 30-year period. Ignoring potential trends within that period when calculating σ, assuming that σ is constant in time and that the sample of 30 yearly values obeys Student's t distribution, the 95% confidence interval for differences in the climatological means is given by $\pm 2(2\sigma^2/30)^{0.5}$, designated here by $\Delta_{95(\mathrm{obs})}$. In several figures to be presented in this paper, horizontal lines showing $\Delta_{95(\mathrm{obs})}$ give a measure of statistically-significant differences compared with the climatological mean during our baseline period, 1990–2010. The measure is closely linked to the statistical tests for the observations, discussed earlier, and can also be applied to past climatological means.

Our third measure is not used directly to assess the significance of the modelled future trends. Instead, it aims to communicate the differences between the recorded inter-annual variability at a single site and the range of unforced

natural climate variability over a larger region. Since potential trends were not removed when calculating σ, it may have an anthropogenic component in addition to natural climate variability. While the recorded fluctuations at a measurement station can be very site-specific, model estimates for internal climate variability portray wider spatial scales. In order to get a rough estimate of the range of unforced natural climate variability in southern Finland, we utilized the findings of Jokela (2011). He examined variations among 49-year averages in a 1200-year simulation, in which the composition of the atmosphere was kept at the pre-industrial level. The simulation was conducted at the Finnish Meteorological Institute using the ECHAM5/MPIOM model (Roeckner *et al*. 2003) with a spatial resolution of about 300 km. Supposing now that the 49-year means follow the normal distribution with a standard deviation, σ_n, there is a 5% probability that the differences between two randomly chosen 49-year means fall outside the interval of $\pm 2^{0.5} 1.96 \sigma_n$ even without any external forcings. Hence, these 95% confidence intervals, labelled here as $\Delta_{95(noise)}$, gave us a measure of model-generated internal climate variability on an inter-decadal time scale. We then calculated the ratio of $\Delta_{95(noise)}$ to the metric of observed range of inter-annual variability, the latter now computed for the 49-year period 1963–2011.This exercise was applied to mean temperature and precipitation in February and July, the two calendar months considered by Jokela (2011).

Temperature

Spatial variations in mean values

The annual mean temperature in southern Finland in 1990–2010 was 4–6 °C (Fig. 1), monthly means ranging from about –7 to –5 °C in February to around 17 °C in July. Located somewhat elevated, the Valkea-Kotinen catchment area is generally cooler than the adjacent lowland lake districts to the east and west. According to Kersalo and Pirinen (2009), both the effective temperature sum, defined as the sum of daily mean temperatures exceeding 5 °C, and the length of the thermal growing season, the period with daily mean temperature above 5 °C, are smaller in the study region than in its surroundings.

The annual mean temperature at station 4 in 1990–2010 was 4.5 °C (Table 3). During 20 years of simultaneous measurements, the temperature at station 3 was on average 0.3 °C lower than at station 4. Similarly, based on a recent six-year period of coincident observations, the temperature at station 2 was 0.7 °C lower than at station 4. Comparable differences were found between station 4 and a grid point representing station 1. However, when considering monthly data at the stations as independent samples, the differences in long-term means appeared not to be significant (Wt test: e.g., stations 3 and 4: $t_{478} = 0.45$, $p = 0.66$). This implies that station 4 describes reasonably well the mean climatological conditions in the Valkea-Kotinen region.

On a daily time scale, however, deviations

Table 3. Seasonal and annual temperatures at station 4. T_{mean} = mean value (standard deviation (σ) of inter-annual variability) in 1990–2010; ΔT = difference between 1964–1989 and 1990–2010 (Wt test's p values in parentheses; *see* Appendix 2 for details); $S_{T,obs}$ = calculated linear regression slope for 1964–2011 (MK test's p values in parentheses; *see* Appendix 1 for details); $S_{T,2040s}$ = projected slope by the 2040s, based on equal weighting of the three GHG scenarios [uncertainty ranges ($\Delta_{90(model)}$) in parentheses]; $S_{T,2080s}$ = projected slopes by the 2080s separately for each scenario (B1, A1B, A2) [uncertainty ranges ($\Delta_{90(model)}$) in parentheses].

	T_{mean} (σ) (°C)	ΔT (p) (°C)	$S_{T,obs}$ (p) (°C/10 yr)	$S_{T,2040s}$ ($\Delta_{90(model)}$) (°C/10 yr)	$S_{T,2080s}$ ($\Delta_{90(model)}$) (°C/10 yr)		
					B1	A1B	A2
Dec–Feb	–5.3 (2.6)	2.4 (0.007)	0.6 (0.09)	0.6 (0.3–0.8)	0.4 (0.2–0.5)	0.6 (0.4–0.7)	0.7 (0.5–0.8)
Mar–May	3.5 (1.1)	0.9 (0.007)	0.4 (0.001)	0.4 (0.1–0.6)	0.3 (0.1–0.4)	0.4 (0.2–0.5)	0.5 (0.3–0.6)
Jun–Aug	15.4 (1.1)	0.5 (0.08)	0.2 (0.03)	0.3 (0.1–0.5)	0.2 (0.1–0.3)	0.3 (0.1–0.5)	0.3 (0.1–0.6)
Sep–Nov	4.5 (1.5)	0.4 (0.3)	0.3 (0.02)	0.3 (0.2–0.5)	0.3 (0.1–0.4)	0.4 (0.2–0.5)	0.4 (0.3–0.6)
Annual	4.5 (0.7)	1.0 (0.0002)	0.4 (0.0002)	0.4 (0.2–0.6)	0.3 (0.1–0.4)	0.4 (0.2–0.6)	0.5 (0.3–0.6)

as large as 4–6 °C were occasionally recorded between station 4 and stations 2–3. Lower daily mean temperatures at station 4 as compared with those at stations 2 and 3 were in a minority, but not infrequent. The largest differences occurred on winter days at temperatures below about –10 °C. For the mean temperature of a single month, the differences ranged from –0.3 °C to 1.2 °C, with a somewhat wider scatter (positive and negative deviations) at temperatures above rather than below about 15 °C.

The notable local-scale variations in weather and climate in that region can largely be explained by the influences of swamps, forests, hills and lakes. In summer, locally-uneven night temperatures are mainly responsible for the spatial variations in monthly and seasonal means. At the most frost-sensitive locations, the air temperature near the ground may sink below zero even in July. The largest diurnal 2-m temperature amplitude in Finland in July was recorded in just this area; on 7 July 1989 the temperature rose from 2.6 °C to 28.5 °C at a station located 12 km to the east of station 3 (Kersalo and Pirinen 2009).

Temporal variations and trends in mean values

There has been a significant warming trend of about 0.4 °C per decade at station 4 since the 1960s (Table 3). This became apparent when examining linear trends in annual means during the whole entire 1964–2011 (MK test; *see* Appendix 1), as well as by comparing climatological (long-term) means during the successive time periods 1964–1989 and 1990–2010 (Wt test; *see* Appendix 2). Furthermore, the same significant increase per decade was obtained both by the seasonal Mann-Kendall method and after fitting a first-order moving average (or ARMA(0,1) model) to deseasonalized and detrended monthly data.

An increase of 0.4 °C per decade was also found in spring temperatures (MK; Table 3 and Appendix 1). In April, the trend slope was even steeper, 0.6 °C per decade (MK: $p = 0.0006$). In summer and autumn, the general warming was less rapid, 0.2–0.3 °C per decade. For these two seasons, the linear trends were significant but the differences between the two sub-periods were not (Table 3 and Appendix 2). The reverse result was obtained for winter. The winter mean temperatures in 1990–2010 were significantly higher than those in 1964–1989, whereas a linear trend for 1964–2011 was not significant (Table 3, Appendices 1 and 2). This resulted from the large inter-annual variability of winter temperatures, including the recent relatively cold winters of 2009/2010 and 2010/2011.

Considering the recent period 1990–2010 at stations 3 and 4, the annual and seasonal trends were not significant. The time interval is evidently too short for the purpose of robust climate change detection. Besides, because of natural variability, climate change is unlikely to proceed at a uniform rate. Temporarily, natural variability may even reverse the direction of the changes from the trend that is expected to result from increases in GHG concentrations. It may be mentioned, however, that an analysis for single calendar months suggested an increase of 1.1 °C per decade (MK: $p = 0.043$) at station 4 in September (Appendix 1).

The historical (prior to 1964) gridded temperature data and climate model simulations can be used to interpret the results. Almost throughout the whole 20th century, the overlapping 30-year annual (middle part of Fig. 2) and spring (not shown) periods were significantly cooler than the respective periods during 1990–2010. The 30-year running winter mean temperatures were also lower for most of the time (bottom part of Fig. 2). By contrast, in summer (top part of Fig. 2) and particularly in autumn (not shown), the differences were chiefly not significant (*see* the confidence intervals $\Delta_{95(obs)}$ in Fig. 2).

The outcome is consistent with the results reported by Tuomenvirta (2004), Tietäväinen *et al.* (2010) and Pirinen *et al.* (2012) for the whole country. We can, therefore, conclude that the temperature changes in the Valkea-Kotinen region followed the past national-scale warming trend in Finland. It is much more difficult to define to what extent the trends detected hitherto can be attributed to the warming influence of the increasing GHG concentrations. This is so because random natural climate variations play a large role at small spatial scales, such as the present study area. Our measure

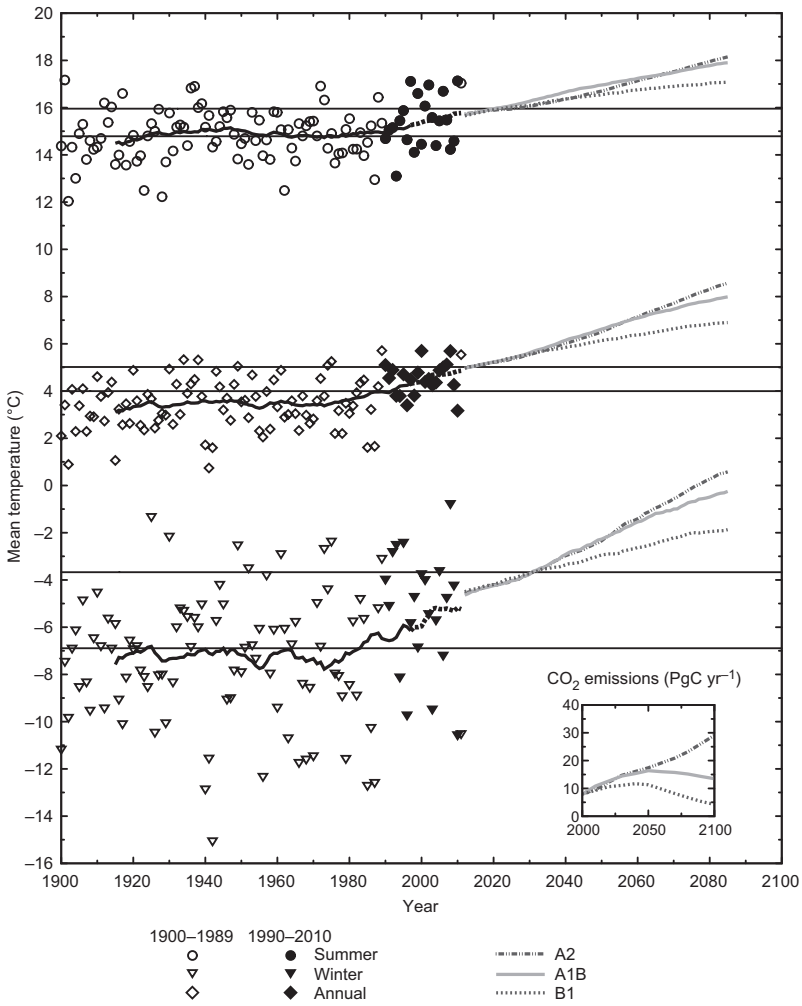

Fig. 2. Observed and projected mean temperatures at station 4 (Lammi Pappila) in summer (June–August; top part), whole year (middle part) and winter (December–February; bottom part) in 1900–2085. The black solid lines depict observed 30-year running means. The horizontal lines indicate 95% confidence intervals $\Delta_{95(obs)}$ for the differences in climatological means (*see* text for details). Multi-model mean projections for the future evolution of the 30-year averages, given separately for three GHG scenarios: SRES A2 (dash-dotted curve), A1B (light grey curve) and B1 (grey dotted curve), are based on the delta change method. The 30-year averages for the period 1998–2011 (black dotted curve) were formed by combining observed recent and projected near-future annual values. The CO_2 emissions corresponding to each temperature scenario are shown in the inset panel.

for spatially-averaged natural temperature variability in southern Finland, $\Delta_{95(noise)}$, appeared to almost match the station-based metric $\Delta_{95(obs)}$ for changes from the current climate. This suggests that a change in mean temperature at a single station might become statistically significant at about the same time as or rather soon after a spatially-averaged mean temperature of a larger region exceeds to the limit of natural climate variability.

A notable anthropogenic contribution to the past changes is supported by the fact that the recorded annual and seasonal mean trends since the 1960s accord remarkably well with model-projected warming in the region during the next few decades (Table 3). The best estimate for the annual mean change by the 2040s is 0.4 °C per decade, the 90% uncertainty interval $\Delta_{90(model)}$ ranging from 0.2 to nearly 0.6 °C per decade. In the 2040s, the average temperature at station 4 would be 6.0–6.4 °C, only weakly depending on the GHG trajectory. The different scenarios actually start to diverge at a longer time horizon (Fig. 2). Based on the multi-model mean estimates, the annual mean temperature in the Valkea-Kotinen region in the 2080s would be 6.9–8.6 °C, the lower end corresponding to the B1 and the higher end to the A2 scenario. By also taking into account the inter-model differences, i.e., $\Delta_{90(model)}$ in Table 3, one can infer that there is a 5% probability for a linear century-scale trend exceeding 0.6 °C per decade if the A2 scenario is realized, or remaining below 0.1 °C per decade according to B1.

The multi-model mean projections suggest that the highest annual mean temperatures experienced thus far in the Valkea-Kotinen region would already become rather typical in the early 2030s (Fig. 2). The mildest winters in the past, with a mean temperature of about –2 °C, and the warmest previous summers, with a mean temperature of about 17 °C, would be illustrative of the 2050s, if the A1B or A2 scenarios were to be realized; in B1, that level of warming would occur two decades later. On the other hand, although the seasonal mean changes are projected to be largest in winter, it may take a couple of decades before the climatological winter temperatures become statistically significantly higher than the mean for 1990–2010. This is visualized in Fig. 2 by the horizontal lines representing $\Delta_{95(obs)}$. The reason is the low ratio of the projected changes in the mean to the recently-recorded inter-annual variations in winter. For the spring mean temperatures, the ratio is almost as high as for the annual means. Significant trends in spring and annual mean temperatures, already recorded in the past, are therefore likely to occur in the near future as well.

Temperature indices

The warming trend in the Valkea-Kotinen area is linked to changes in various climatic indicators. Our first example deals with the occurrence of days with a mean temperature below or above 0 °C, designated here as cold and mild days, respectively. Based on the trend analysis (MK: $p = 0.006$; *see* Appendix 1), and on comparisons of average values at station 4 between 1964–1989 and 1990–2010 (MW, $p = 0.02$; *see* Appendix 3), the annual number of cold days declined by about five (4%) per decade. The maximum length of cold spells in winter was also reduced by about five days (12%) per decade (MK: $p = 0.027$). In contrast to the majority of the temperature variables we considered, the longest period of consecutive mild days within a year did not indicate significant changes during 1964–2011, but did, however, during 1990–2010 when it extended by almost two weeks (7%) per decade (MK: $p = 0.014$).

The most coherent changes in the indices occurred in April. The linear trend in the number of cold days for that calendar month within the period 1964–2011 was –1.4 days (–22%) per decade ($p = 0.007$), and as distinct as –3 days (64%) per decade ($p = 0.010$) in 1990–2010. Concurrently, the maximum length of consecutive cold-day spells in April decreased by 0.6 days (–16%) per decade ($p = 0.017$) in 1964–2011 and by 2 days (–64%) per decade ($p = 0.050$) in 1990–2010. The longest uninterrupted period of mild days increased in turn by 2 days (12%) per decade ($p = 0.005$) in 1964–2011 and by 7.5 days (40%) per decade ($p = 0.009$) in 1990–2010. Besides the MK test results given above (*see* also Appendix 1), similar results for April were given by the MW test for the two successive periods (Appendix 3).

These observed changes in spring are consistent with the projections for earlier onsets of the thermal spring and the growing season in the future (e.g., Ruosteenoja *et al*. 2011, Laapas *et al*. 2012). The decreasing wintertime trend in the cold spells also agrees with the model projections. For example, frost days are expected to become less frequent and *vice versa* for wintertime thaw events (Jylhä *et al*. 2008, Vajda *et al*. 2011, Laapas *et al*. 2012).

As regards summer conditions, the annual maximum temperature at station 6 (Fig. 1) had a long-term average of 28.7 °C (SD = 1.7 °C) with no significant trend during either 1928–2010 or 1961–2010 (MK tests). Likewise, the annual number of days with maximum temperatures above 23 °C or 27 °C at that station did not change significantly during either period. Similar results have been obtained also for other areas in Finland. According to Tietäväinen *et al*. (2012), at 30 stations in 1961–2010, annual maximum temperatures and annual numbers of days with maximum temperatures above 23 °C, or 27 °C, more commonly had a positive rather than a negative linear regression slopes, but in most cases the tendencies were not statistically significant.

In connection with the so-called the 2010 Russian heat wave (Otto *et al*. 2012), an unusually high temperatures were measured in our study region on 28 July 2010: 34.6 °C at station 2 and 33.0 °C at station 4. On the following day, a new national temperature record of 37.2 °C

was measured in Joensuu, eastern Finland (Saku *et al*. 2011). At station 6, by contrast, the 2010 maximum of 32.8 °C was equal to the previous maximum measured in 1933. This highlights the importance of analyzing sufficiently long time series of observations. Based on the GEV and GPD analyses of the data from station 6 until now, the return period of 32.8 °C is about 150 years (corresponding to an annual probability of about 0.7%) with a 95% confidence interval from 30–40 years to several centuries. Nonetheless, with climate change continuing, a marked increase in the probability of very high temperatures can be expected (e.g., Nikulin *et al*. 2011, Coumou *et al*. 2013, Morak *et al*. 2013).

The projected warming in May and September implies that during the next few decades, the climatic type of the Valkea-Kotinen region, according to the Köppen classification system, would change from the current boreal subtype Dfc to Dfb; that subtype is characterized by longer summers than those in Dfc. As a result of the projected increases in the February mean temperature, a transfer from the main category D to another main category, designated by C (temperate), would take place in the 2060s under the A1B and A2 scenarios or, according to B1, not until the end of the 21st century. In category C (D), the average temperature of the coldest month is above (equal to or below) –3 °C (e.g., Jylhä *et al*. 2010).

Precipitation

Located in an upland area, the Valkea-Kotinen area is not only cooler but also wetter than its surroundings. For example, at station 6, sited in a lowland area, the average precipitation sum is typically about 50 mm smaller than at station 4 (Pirinen *et al*. 2012). Precipitation data at the latter station appeared to be climatologically representative for the Valkea-Kotinen region, without any significant differences in the long-term means compared to station 3 (MW, $n = 240$, $Z = 0.17$, $p = 0.87$). For single annual, monthly and daily sums, however, differences as large as about ±40 mm, ±30 mm and ±20 mm, respectively, or even greater, were occasionally encountered.

In contrast to mean temperature, we could not discover any significant long-term trends in annual or seasonal mean precipitation, but only large year-to-year variations (Table 4 and Fig. 3). The only calendar months with increases in precipitation in 1964–2011 were January (MK: $p = 0.028$) and June (MK: $p = 0.005$; *see* Appendix 1 for details). Linear slopes during the period 1990–2010 were insignificant for all seasons and months. The results are consistent with those of Ylhäisi *et al*. (2010) for May–September rain in an area around station 8 since 1908; the long-term trends varied in sign from month to month.

In the future, based on the multi-model mean estimates under the three emission scenarios, the average annual precipitation sum is likely to grow at a rate of 1%–2% per decade throughout this century (Table 4). The rate corresponds to an increase from the observed mean of 635 mm in 1990–2010 to about 670 mm in the 2040s and to about 700–735 mm in the 2080s. The mean annual precipitation sum in the 2040s would significantly exceed the contemporary climatological mean. The wettest year at station 4 so far, 1981 (851 mm), however, would be considered wet in the future as well. Even if the A2 scenario were to become true, there would be only a 5% probability that the 30-year mean annual total exceeded 800 mm (*see* $\Delta_{90(\mathrm{model})}$ in Table 4).

The future changes in precipitation are expected to be strongest in winter, both in relative and absolute terms. Under the A2 scenario, the linear century-scale winter trend would be about 3% per decade; for the other scenarios 1%–2% per decade (Table 4). A comparison of the projections with the recently observed year-to-year variations suggests that the wintertime increases will exceed the limit of statistical significance during the latter half of this century, but that this is unlikely to happen to the summer mean precipitation ($\Delta_{95(\mathrm{obs})}$ in Fig. 3). The 90% uncertainty intervals for the model projections reveal that the summer precipitation sum might even decrease (*see* $\Delta_{90(\mathrm{model})}$ in Table 4). Despite that, precipitation amounts will on average remain more abundant in summer and autumn than in winter and spring. In occasional years, however, winter totals may exceed summer accumulations; this has also occurred earlier (Fig. 3).

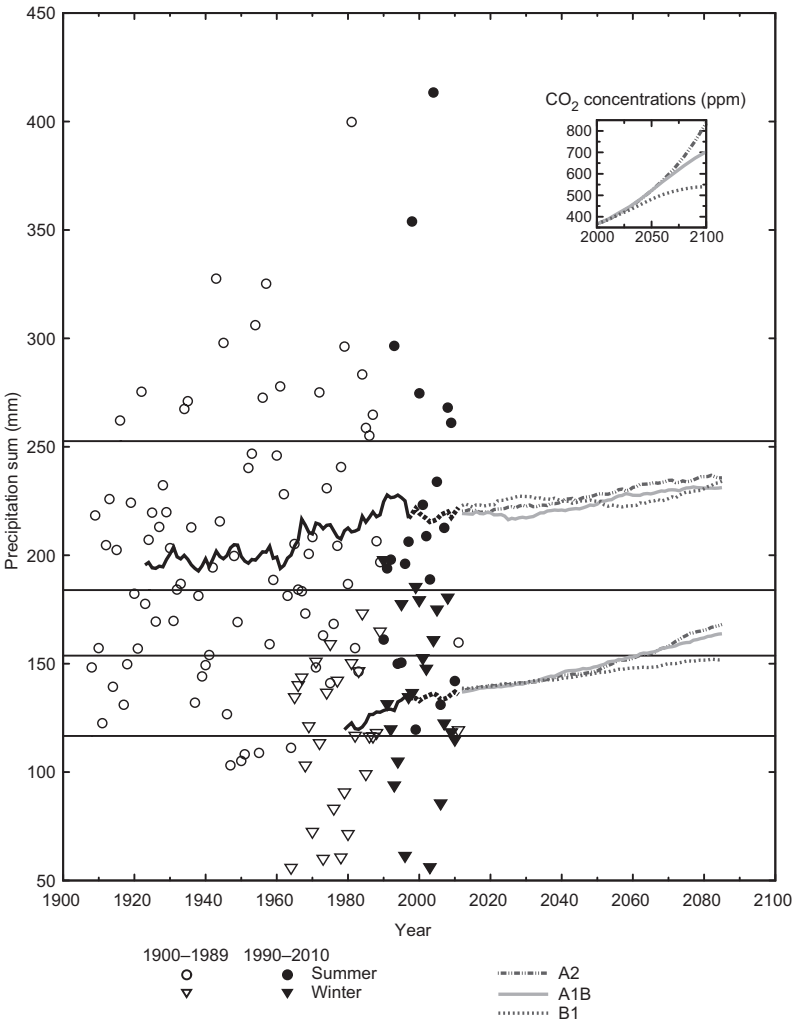

Fig. 3. Observed and projected precipitation sums at station 4 in summer (June–August 1909–2085; top part) and in winter (December–February 1964–2085; bottom part). Horizontal lines indicate 95% confidence intervals, $\Delta_{95(obs)}$, for differences in climatological means (*see* text for details and Fig. 2 for more explanations).

Table 4. Seasonal and annual precipitation at station 4. P_{mean} = mean value (standard deviation (σ) of inter-annual variability) in 1990–2010; ΔP = difference between 1964–1989 and 1990–2010 (MW test's p values in parentheses); $S_{P,obs}$ = calculated linear regression slope for 1964–2011 (MK test's p values in parentheses); $S_{P,2040s}$ = projected slope by the 2040s, based on equal weighting of the three GHG scenarios; $S_{P,2080s}$ = projected slopes by the 2080s separately for each scenario (B1, A1B, A2).

	P_{mean} (σ) (mm)	ΔP (p) (mm)	$S_{P,obs}$ (p) (%/10 yr)	$S_{P,2040s}$ ($\Delta_{90(model)}$) (%/10 yr)*	$S_{P,2080s}$ ($\Delta_{90(model)}$) (%/10 yr)*		
					B1	A1B	A2
Dec–Feb	135 (40)	18 (0.1)	5 (0.1)	2 (0 to 3)	1 (1 to 2)	2 (1 to 4)	3 (2 to 4)
Mar–May	108 (30)	2 (0.6)	0 (1.0)	1 (–1 to 3)	1 (–0 to 3)	2 (0 to 3)	2 (0 to 3)
Jun–Aug	218 (74)	7 (0.8)	3 (0.3)	1 (–1 to 3)	1 (–0 to 2)	1 (–1 to 2)	1 (–1 to 3)
Sep–Nov	174 (48)	–9 (0.6)	0 (0.9)	1 (–0 to 3)	1 (0 to 2)	1 (0 to 2)	2 (0 to 3)
Annual	635 (74)	17 (0.5)	1 (0.2)	1 (0 to 2)	1 (0 to 2)	2 (1 to 2)	2 (1 to 3)

* In parentheses are the uncertainty ranges ($\Delta_{90(model)}$) due to scatter among the model projections.

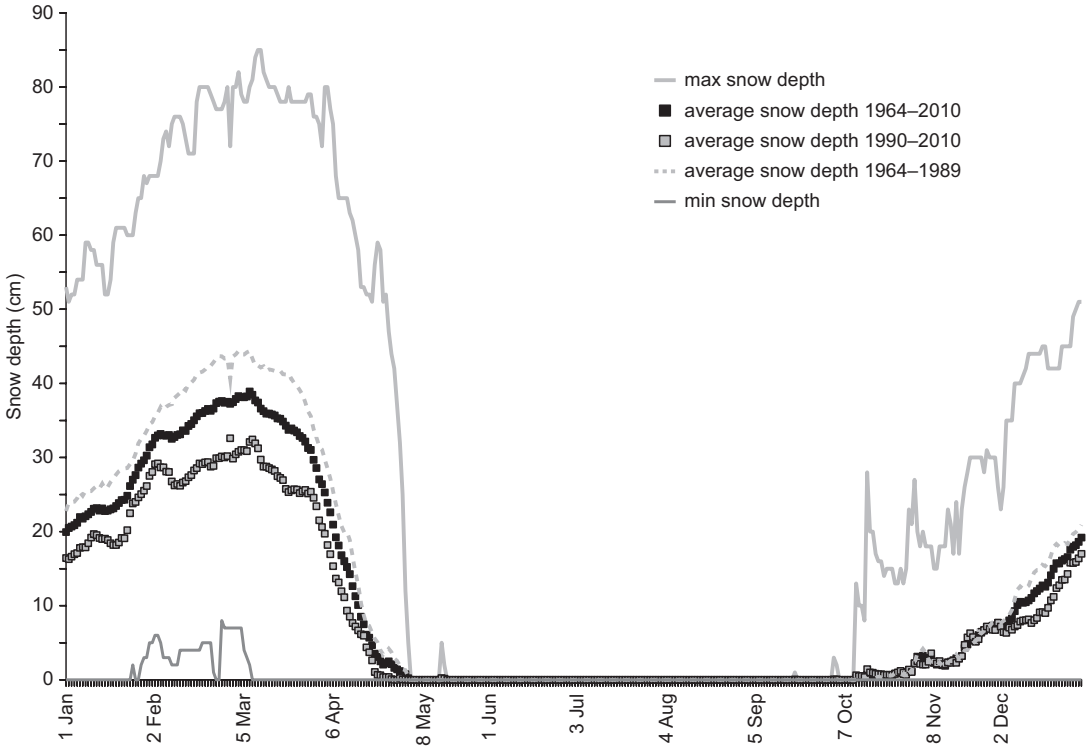

Fig. 4. Temporal evolution of daily snow depth in the course of the year at station 4. In addition to average values for 1964–2010 (black squares), 1964–1989 (dashed curve) and 1990–2010 (grey squares), the highest and lowest values in 1964–2010 are shown.

The observations in the past and the model projections for the future both imply that changes in the mean precipitation will become statistically significant far more slowly than those in temperature. Besides, changes at a single station are likely to exceed the limit of statistical significance at a later stage as compared with means over a large area, like southern Finland. This was suggested by a comparison between $\Delta_{95(obs)}$ and $\Delta_{95(noise)}$ for precipitation; the latter was clearly smaller.

In addition, we briefly examined forms of precipitation. Based on visual observations at station 8 in 1980–2009, about 72% of the annual precipitation there typically falls in the liquid phase, 17% in the solid phase and 11% as a mixture of both. In December–March the share of snowfall is about half and the portion of sleet almost 30%. In November and April, the share of rain is about half and the rest is equally partitioned into snow and sleet. In the future, increases in temperature will alter these patterns: based on simple physical reasoning, the fractions of rain and sleet will increase at the expense of snow.

Snow depth

The cooler and wetter climate of the Valkea-Kotinen area, as compared with that of its neighbourhood, also implies a deeper snow cover. Over at least a four-week interval, starting at the end of January, snow was on the ground in every winter during 1964–2011 (Fig. 4). The deepest snow cover in the region was measured on 9–13 March 1984. At that time, the depth was 81–85 cm at station 4 (Fig. 4) and even as much as 108 cm at a distance of 15 km to the northeast, at a station no longer operating. The climatological representativeness of snow measurements at station 4 can be considered adequate. Based on comparisons between station and gridded data, the snow depth on 15 March was on

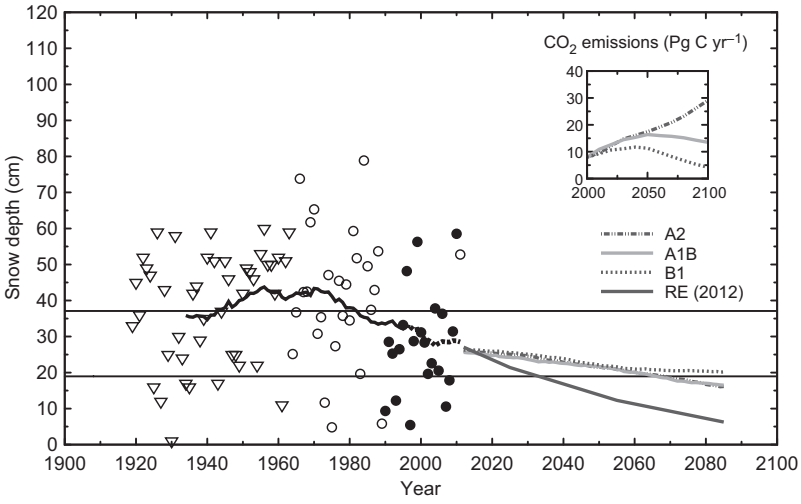

Fig. 5. Observed and projected mean snow depths at station 4 on 15 March in 1919–1963 (▽), and in March since 1964 (○). The filled circles (●) denote measurements in 1990–2010. The solid dark-grey line, denoted by RE (2012), shows projected changes in southwestern Finland at (60.9°N, 23.4°E) in the regional-model based analysis of Räisänen and Eklund (2012) for the A1B scenario (*see* text for details). For the other line meanings, *see* Fig. 2.

average 4 cm (10%) deeper around station 1 than station 4, which is not significant according to the MW test ($Z = -1.1$, $p = 0.26$).

The first snow often falls at station 4 around 1 November, and the seasonal permanent snow cover, defined as the longest unbroken period of at least 1 cm of snow, arrives about a month later. In occasional years, snow depth has already exceeded 15 cm for a short while in October (Fig. 4). The tendencies towards later onsets of the first and permanent snow cover, as well as towards less November snow cover were relatively weak in comparison with the large inter-annual variability. Instead, the change in average December–February snow depth was significant (MW: $p = 0.029$; *see* Appendix 3), the depth being 8 cm (28%) smaller in 1990–2010 than in 1964–1989. A decrease in February snow depth of 4 cm (11%) per decade during 1964–2011 was also significant (MK: $p = 0.046$; *see* Appendix 1).

The snow cover is typically thickest in March (Fig. 4). In 1990–2010 it was on average 13 cm thinner at this time than in 1964–1989 (MW, $p = 0.011$). Furthermore, the average spring snow depth was 6 cm less (MW, $p = 0.015$) (and the average annual mean snow depth 3–4 cm less; MW, $p = 0.010$). Snow melted away slightly earlier than previously (Fig. 4), but the shift was not significant. The same is true for the duration of the permanent snow cover: the reduction in the mean from 129 days in 1964–1989 to 118 days in 1990–2010 was minor as compared with the inter-annual standard deviation of 32 days.

Gridded snow depth data on 15 March was used in Fig. 5 as a proxy for monthly average snow depth in 1919–1963. This was justified by the high correlation coefficient (0.97, $p < 0.0001$), the negligibly small mean difference (0.6 cm) and the small root mean square error (4.5 cm) between the two snow variables at station 4 in 1964–2011. It appeared that snow depth on 15 March tended to increase in the Valkea-Kotinen region during the first half of the 20th century, although the upward linear trend was not statistically significant. A gentle turn towards thinner snow cover in March occurred in the 1960s onwards, as an indicator of the warming trend.

In the future, reductions in the snow cover are projected to continue. Based on the global climate model simulations used in this paper (Table 2), the average liquid water content of snow in March would diminish by 5% per decade throughout the 21st century under the A1B and A2 scenarios, or by 3%–4% per decade in the case of the B1 scenario (Fig. 5). Similar percentage reductions are to be expected in February and January, while at the beginning and end of the snow season the projected changes are up to twice as large, implying a tendency towards shorter snow periods in the future (*see* also Holmberg *et al*. 2014). Compared with the recently-observed year-to-year variations, however, the changes are projected to exceed the limit of statistical significance earlier in the future in winter than in autumn and

spring. On the other hand, these findings may be underestimates. According to Räisänen and Eklund (2012), the rate of snow water equivalent decrease in March would be about twice as much as the figures above. Several global models systematically simulate too cold present climate conditions, which tends to reduce the diminishing trend of snow water equivalent. In the ensemble of regional climate models analysed by Räisänen and Eklund (2012), this bias is small. For the sake of comparison, their results based on regional climate model simulations are also shown in Fig. 5. Depending on which one of the scenarios will turn out to be closer to the truth, the changes could surpass the limit of statistical significance as early as the 2030s or, on the other hand, not until the latter half of this century (*see* $\Delta_{95(obs)}$ in Fig. 5 for March).

Lake ice cover

Our last example of indicators of the warming trend deals with lake ice. On average, three weeks before the onset of the seasonal snow cover at station 4, Lake Valkea-Kotinen, on the shore of which station 1 is located (Fig. 1), becomes completely frozen. In 1990–2011 the average freezing date of the lake was 15 November. The average length of the ice-season was 167 days, i.e., 5.5 months, the breakup occurring around 30 April (Fig. 6). The inter-annual variability, as measured by the standard deviation, was larger for ice-on (65 days) than for ice-off (25 days). The earliest freezing date, 18 October, was recorded in 2002 and the latest one, 21 December, in 2000. In spring the earliest breakup took place on 14 April in 2007 and latest on 9 May in 1997.

Being linearly correlated with the mean temperature in April ($r = –0.77$, $p < 0.0001$) and the duration of the longest mild spell during that month ($r = –0.56$, $p = 0.008$), the date of ice-off became earlier by 6 days per decade (MK: $p = 0.002$; *see* Appendix 1). Simultaneously, the length of the ice-season decreased by 17 days per decade (MK: $p = 0.009$). In the future, according to Holmberg *et al*. (2014), the ice-season on the lake is likely to shorten at approximately the same rate.

In contrast to the ice-off day and the duration of the ice period, the trend in the ice-on day did not prove to be significant. This is consistent with the fact that the freezing time of the lake was strongly correlated with the November air temperature indices, e.g., the number of cold days ($r = –0.84$, $p < 0.0001$) and the duration of mild spells ($r = 0.80$, $p < 0.0001$) at station 4, but these indices did not reveal any significant trends.

Weyhenmeyer *et al*. (2004) showed that in Sweden the relationship between the timing of lake-ice breakup and air temperature can actually be nonlinear. They explained that this was a result of marked differences in the response of the timing of lake-ice breakup to changes in air temperature between colder and warmer geographical regions (or between colder and warmer years). In accordance with that, we can assume that if the mean air temperatures in the coldest months of the year are only slightly below the freezing point, even minor shifts in temperature may cause major changes in ice-on and ice-off days. Besides, according to Ruosteenoja (1986), precipitation falling in liquid form somewhat contributes to lake ice breakup. By growing the portion of rain and sleet at the expense of snow, increases in air temperature will thereby advance the timing of ice breakup also indirectly.

Wind speed

Throughout the year, forests are vulnerable to the direct and indirect impacts of high wind speeds (e.g. Peltola *et al*. 2010, Jönsson and Bärring 2010, Gregow *et al*. 2011). Besides, during the ice-free season windiness affects processes in lakes (*see* e.g., Holmberg *et al*. 2014). Because of the short period of wind data at station 2, three more distant stations were consulted as well. Based on 3-hourly measurements of 10-minute average wind speeds since 2006, station 2 is significantly less windy (MW: $Z = –8.7$, $p < 0.0001$) than stations 5 (Asikkala) and 8 (Jokioinen) and more windy (MW: $Z = 9.5$, $p < 0.0001$) than station 7 (Lahti) (*see* Fig. 1 for the locations). The different surroundings of the measuring sites, ranging from a sheltered garden (station 5) via a forest (2) to broad fields (8) and open lake

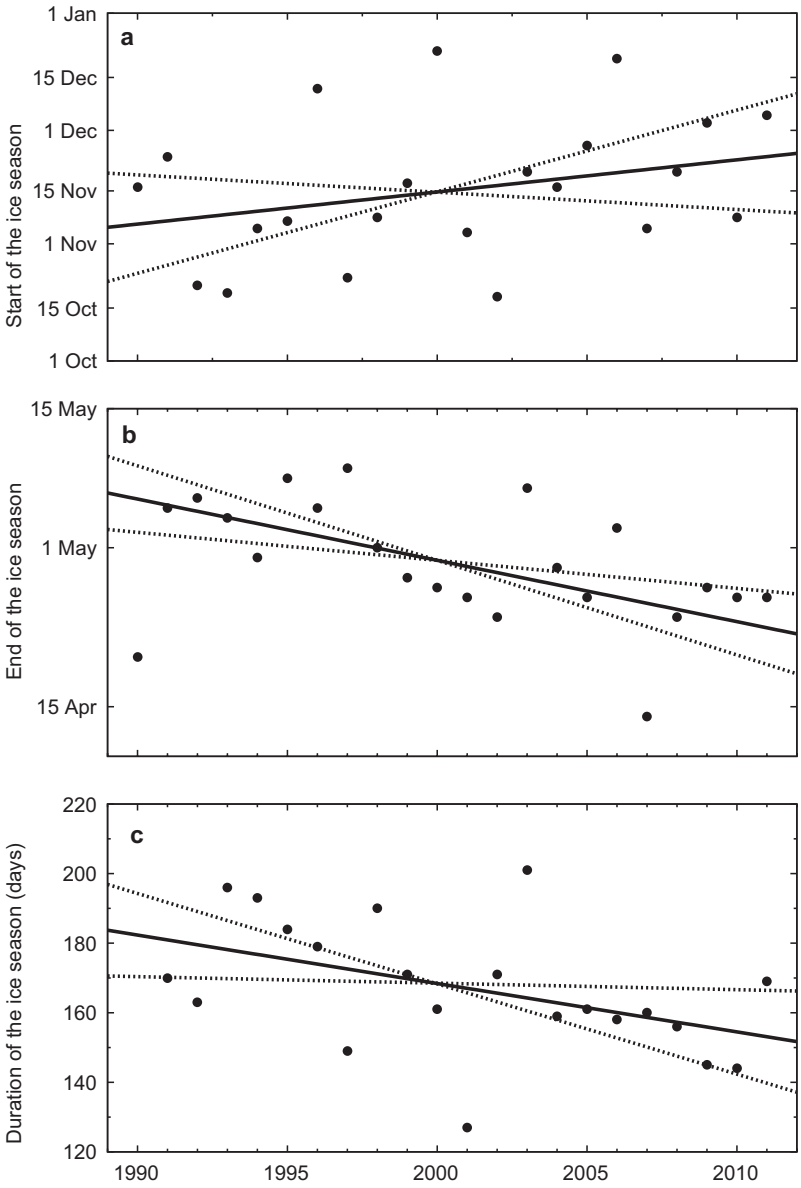

Fig. 6. Ice cover on Lake Valkea-Kotinen in 1990–2011. (**a**) Date of ice-on, defined as the day when the lake was completely frozen and did not melt until the following spring. (**b**) Date of ice-off, defined as the day when > 50% of the lake area was free of ice. (**c**) Length (number of days) of the ice season. Linear regressions (solid line) with uncertainty ranges (dotted lines) are also shown.

areas (7), clearly affect the wind conditions. At 3–15 metres above the tree tops, the average wind speed at station 2 in 2006–2011 was 2.3 m s^{-1}, which differed from the corresponding 6-year averages at the other stations by about 1 m s^{-1}. A comparison between the frequency distributions of the 3-hourly data revealed that for wind speeds exceeding a threshold of about 6 m s^{-1}, station 8 was more characteristic of station 2 than the remaining two. Moreover, that station has the longest times series. Accordingly, we mainly focus on station 8.

The wind climate is characterized by lower mean wind speeds in summer than in the other seasons. Compared with the average annual mean of wind speed of 3.7 m s^{-1} at station 8 in 1959–2010 (or 3.5 m s^{-1} in 1990–2010), monthly mean values were 0.1–0.5 m s^{-1} lower in June to September and 0.2 m s^{-1} higher in November and December. Apart from insignificant changes in January and February, the monthly, seasonal and annual mean winds weakened at a rate of 0.1 m s^{-1} (or 0.2 m s^{-1} in April) per decade during the period 1959–2010 (MK: p ranging from less

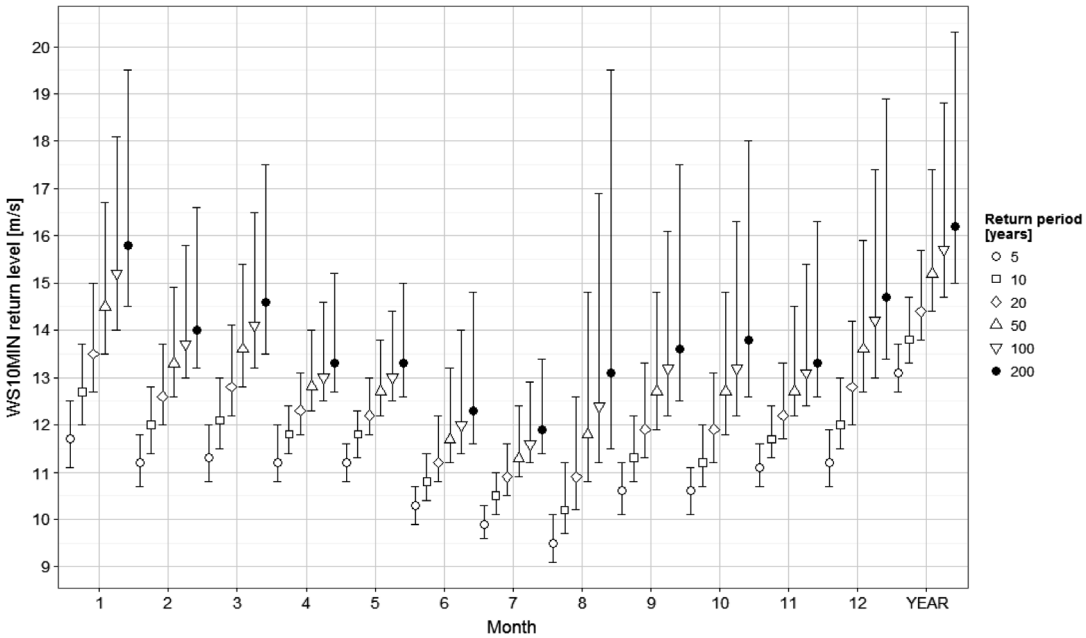

Fig. 7. Return levels of 10-minute average wind speed (m s^{-1}) at station 8 based on observations in 1959–2010. The return levels corresponding to 5-, 10-, 20-, 50-, 100- and 200-year return periods are given separately for each calendar month as well as for the whole year. The symbols express maximum likelihood estimates of the return levels and the vertical lines show 95% confidence intervals based on the profile likelihood method (*see* text for details).

than 0.0001 to 0.04; *see* Appendix 1). However, during the shorter period of 1990–2010 the negative trends were not significant.

In contrast to the averages of the 10-minute mean winds, the monthly and annual maxima generally had rather stationary time series in 1959–2010. The average annual maximum was 12 m s^{-1}. Only in March (MK: $p = 0.004$) and June (MK: $p = 0.003$) had the maxima weakened at a rate of 0.3–0.4 m s^{-1} per decade (*see* Appendix 1). This allowed us to perform extreme value analysis for the wind data in 1959–2010 by using time-independent GEV-distributions.

The maximum likelihood estimate for the 20-year return level of the 10-minute average annual maximum wind speed at station 8 was 14.4 m s^{-1}, with the confidence intervals of 13.8–15.7 m s^{-1} (Fig. 7). During the period 1959–2010 the highest 10-minute average wind speed at station 8 was 16 m s^{-1}, observed on 31 January 1997. On that date strong gusty winds occurred in southern Finland as the result of a strong low-level jet (Myllys 1999). According to the GEV distribution fitted to the data, the return period of such a high wind speed would be more than 100 years (Fig. 7). Nonetheless, if the confidence intervals are also taken into account, one may argue that the return period of 16 m s^{-1} could be shorter, about 50 years.

During the open-water season from May to November, the probability of 10-minute winds exceeding 10 m s^{-1} was smallest in June to August (Fig. 7). In August, however, there is a large uncertainty in the return levels. This ensues from the fact that the shape parameter of the GEV distribution fitted to the maxima in August was ambiguous in sign, with a maximum likelihood estimate close to zero but having wide error limits.

In the future, based on the 9-model mean projections (Table 2), the annual average wind speed at station 8 would increase by about 1% by the 2040s and by about 1%–2% by the 2080s. The largest increases in monthly means, 2%–4% (or 0.1 m s^{-1}) by the 2040s, would occur in January and February. During the open-water season, the projected changes are generally very small. Only in September and November would an increase of 1%–2% occur by the 2040s. These results imply that the past negative trends,

already statistically insignificant in 1990–2010, would gradually level out and slowly turn positive. By the 2080s under the A1B scenario, the multi-model mean changes in January and February mean wind speeds would be 4%–5%, with a winter mean change of 3%–4%. These increases do not reach $\Delta_{95(obs)}$, suggesting that they are rather modest as compared with the recent variations in observed wind.

Accompanying the gentle increases in average winds, extreme wind speeds are likely to slightly intensify as well. Based on research by Gregow *et al*. (2012), annual maximum wind speeds would increase by 1%–2% in the southwestern part of Finland by 2081–2100, but not yet by 2046–2065. More frequent high wind speeds in northern Europe in the future are likewise envisaged by Nikulin *et al*. (2011) and Harvey *et al*. (2012).

Solar radiation

Finally, we briefly consider total (or "global") solar radiation, i.e., the sum of direct and diffuse (or scattered) irradiance on a horizontal surface, at station 8. Based on 3-hour measurements in 1990–2009, the solar radiation energy received during the whole year was on average 3434 MJ m^{-2} (or 3412 MJ m^{-2} in 1980–2009), with a percentage standard deviation (σ) of 5%. The largest monthly mean energy amounts, about 590 MJ m^{-2} (σ = 12%), were received in June and July, and the smallest morsel, 16 MJ m^{-2} (σ = 22%), in December. The portion of the solar energy obtained as diffuse radiation was on average 46% for the annual sum but as large as about 70%–75% in November to January.

During 1980–2009, the annual direct radiation was enhanced by 112 MJ m^{-2} (6%) per decade (MK: p = 0.002; *see* Appendix 1). This trend was provided by an intensification of direct radiation in spring by 50 MJ m^{-2} (8%) per decade (p = 0.010) and in autumn by 27 MJ m^{-2} (15%) per decade (p = 0.008). In contrast, diffuse radiation weakened in all seasons but autumn. The trend in the annual diffuse radiation was –70 MJ m^{-2} (–4%) per decade (p = 0.00003), the declines in summer being the most notable in absolute terms (–32 MJ m^{-2} per decade, p = 0.0004) and those in winter in relative terms (–7% per decade, p = 0.003). In autumn, the total solar radiation increased by 20 MJ m^{-2} (5%) per decade (p = 0.050). The negative trend in annual diffuse radiation and the positive trend in spring direct radiation were statistically significant even for the short period of 1990–2009 (*see* Appendix 1).

A decrease in mean annual solar radiation of 8.7% at station 8 during the period from 1958 to 1992, reported by Heikinheimo *et al*. (1996), corresponded to a trend of –1.7% per decade, and was mainly attributed to a pronounced increase in cloudiness, with only a minor contribution from the direct effects of the relatively large aerosol load at that time. The trends in annual direct (diffuse) radiation of 6% (–4%) per decade from 1980 to 2009, observed here, may likewise mainly ensue from changes in cloudiness. On the other hand, the past evolution in solar radiation at station 8 is qualitatively consistent with the observed European-scale "dimming" from the 1950s to the 1980s, followed by a partial recovery ("brightening") thereafter. Whereas this progression has largely been explained by the at first growing and then declining amounts of aerosols in the atmosphere over the continent (Wild and Schmucki 2011), the projected changes in the future are predominantly of meteorological origin (Ruosteenoja and Räisänen 2013). Potential major volcanic eruptions would naturally affect these trends.

Based on the 18-model mean estimates (Table 2), wintertime solar radiation in southwestern Finland would weaken by 6% by the 2040s. Relative to $\Delta_{95(obs)}$, the decrease would be statistically significant one or two decades later. In the course of time, the winters turn increasingly dark due to the reduction of solar radiation. If the A1B or A2 scenarios materialized, corresponding to a weakening of 12%–14% in wintertime insolation by the 2080s, typical winters at that time would resemble the fifth or sixth darkest winters during the last three decades. Compared to winter, the projected percentage negative trends in spring and positive trends in autumn are more modest.

Synthesis of the results

The findings of this study are summarized in

Table 5. Depending on the significance levels, the trends are divided into four classes: $p < 0.001$, $0.001 < p \le 0.01$, $0.01 < p \le 0.05$ or $p > 0.05$. In the classification of past tendencies, we used the calculated linear slopes as a primary criterion and (except for solar radiation) the differences in means between two successive periods as a secondary measure. The confidence class based on the secondary criterion is shown in parallel with those cases in which the two measures disagreed on whether the limit $p = 0.05$ is attained.

For the future trends, the emphasis is put on the multi-model mean projections under the A1B scenario. The statistical significance of the changes was evaluated in relation to the observed inter-annual variability, given by $\Delta_{\%}$(obs), where

Table 5. A summary of the statistical significance of the observed past trends and projected future changes in climate variables in the Valkea-Kotinen region under the A1B scenario: increase with $0.01 < p \le 0.05$ (↑), $0.001 < p \le 0.01$ (↑↑) or $p \le 0.001$ (↑↑↑); decrease $0.01 < p \le 0.05$ (↓), $0.001 < p \le 0.01$ (↓↓) or $p \le 0.001$ (↓↓↓); not statistically significant (~), not relevant (empty). The following three additional notations are used: (1) A pair of codes separated by a forward slash, e.g., (~/↑), for a past period indicates that the following two measures disagree on whether $p \le 0.5$ or $p > 0.5$: (i) linear slope across the whole period (the left-hand side); (ii) difference between the means in the former and latter half of the period (the right-hand side). (2) Arrows in bold for a future time span indicate that the multi-model mean change in terms of observed inter-annual variability is statistically significant and, in addition, there is a high agreement among the models on the sign of the change, as indicated by $\Delta_{90(\text{model})}$ (*see* Tables 3–4). (3) A pair of codes for a future time span designates statistical insignificance in terms of observed inter-annual variability but a high inter-model agreement regarding an increase (~/↑) or a decrease (~/↓). Note that all projections are given relative to the mean of the period 1990–2010.

		Confidence levels of the changes				
Variable	Time span	Dec–Feb	Mar–May	Jun–Aug	Sep–Nov	Annual
Mean temperature	1964–2011	~/↑	↑↑	↑/~	↑/~	↑↑↑
	2040s	**↑↑↑**	**↑↑↑**	**↑↑↑**	**↑↑↑**	**↑↑↑**
	2080s	**↑↑↑**	**↑↑↑**	**↑↑↑**	**↑↑↑**	**↑↑↑**
Number of days < 0 °C	1964–2011	~/↓	~		~	↓↓
Length of spell < 0 °C	1964–2011	↓	~		~	~/↓
Length of spell > 0 °C	1964–2011	~	↑/~		~	~
Mean precipitation	1964–2011	~	~	~	~	~
	2040s	~/↑	~	~	~	**↑**
	2080s	**↑↑↑**	↑↑	~	**↑**	**↑↑↑**
Wind speed	1959–2010	↓/~	↓↓↓	↓↓↓	↓↓↓	↓↓↓
	2040s	~	~	~	~	~
	2080s	~	~	~	~	~
Direct solar radiation	1980–2009	~	↑	~	↑↑	↑↑
Diffuse solar radiation	1980–2009	↓↓	↓↓↓	↓↓↓	~	↓↓↓
Global solar radiation	1980–2009	~	~	~	↑	~
	2040s	**↓**	~	~	~	~
	2080s	**↓↓↓**	**↓**	~	~	~
Snow depth	1964–2011	~/↓	~/↓		~	↓
	2040s	**↓↓**	~/↓		~/↓	**↓**
	2080s	**↓↓↓**	**↓↓**		**↓**	**↓↓↓**
		Date of snow-on	Date of snow-off		Date of first snow	Duration
Snow season	1964–2011	~	~		~	~
			Date of ice-off		Date of ice-on	Duration
Lake-ice season	1990–2011		↓↓		~	↓↓

% = 95, 99 or 99.9. Scatter among the models was additionally taken into account by considering the uncertainty range $\Delta_{90(model)}$ and using different styles for the arrows in Table 5. The more robust the future changes are, the thicker arrows appear. Since we did not explicitly study the uncertainty range $\Delta_{90(model)}$ for snow, wind speed and solar radiation, here we made use of fig. 5 in Räisänen (2008), figs. 8–9 in Räisänen and Eklund (2012), figs. 3–4 in Gregow *et al*. (2012) and fig. 2 in Ruosteenoja and Räisänen (2013).

Based on the combinations of the detected past and expected future changes in the seasonal and annual means, the trends for the Valkea-Kotinen region may further be classified into the following four main categories:

A: A significant trend hitherto is expected to continue during the 21st century. The exact rate of the future changes depends on the evolution of the GHG concentrations. The following trends belong to this category: increases in annual and spring mean temperature, decreases in annual mean snow depth and, inferring from the projections by Holmberg *et al*. (2014), the length of the lake-ice season and the earlier melting of lake ice.

B: The observed tendency hitherto is not yet indisputably statistically significant but it is likely to become so (i) by the 2040s or (ii) by the 2080s. Increases in winter, summer and autumn temperature, increases in annual precipitation, decreases in winter mean snow depth and winter mean incident solar radiation belong to B(i). Increases in winter, spring and autumn precipitation, decreases in spring and autumn mean snow depth and in spring solar radiation belong to B(ii). Inferring again from the projections by Holmberg *et al*. (2014), the onset of the lake-ice season is also included in the B category.

C: A significant trend hitherto levels out and becomes statistically insignificant. Changes in autumn solar radiation as well as seasonal and annual mean wind speed belong here.

D: Both past and future trends are unclear in sign or weak in comparison to the recently-observed inter-annual variability. This applies to summer precipitation, summer solar radiation, and annual solar radiation.

Expectedly, the B1 scenario implies a slower and the A2 scenario a more rapid surpassing of the limit of statistical significance than the A1B scenario considered in here. For example, future decreases in the annual mean solar radiation would become statistically significant by the 2080s under the A2 scenario, but not in the B1 or A1B scenario. If the results of Räisänen and Eklund (2012) are taken into account, the decreases in spring and autumn mean snow depth would be classified as the type B(i) instead of B(ii).

The above categorization focuses on the multi-model mean projections. If the changes were to be assumed to take place more slowly, following the lower end of the inter-model uncertainty interval $\Delta_{90(model)}$ rather than the middle estimate, there would be less variables in categories A and B(i), and more variables in B(ii) and D. Evidently, for the upper end of the inter-model range, the opposite would be implied. The 95th percentile of the model projections would suggest a significant increase in total precipitation for summer, too.

Conclusions

The primary purpose of this work was to support climate-change impact, adaptation and vulnerability (IAV) studies related to ecosystems in the Valkea-Kotinen environmental monitoring area. Focusing on climate in that region, we used data from only a few, one to four, weather stations for each climate variable of interest. The small number of stations does no allow for generalizing the observational-based results for the whole southern part of the country. It also directed us to concentrate on variables that are spatially rather uniform. For example, studies into heavy precipitation events would have required data from a larger number of stations. This also holds for a robust detection and attribution of anthropogenic climate change, as well as for a careful analysis of relationships between different variables and between trends in them. Instead, it is clear that the scenarios presented here for future climate change are appropriate on a wider spatial scale than the Valkea-Kotinen region alone.

The Valkea-Kotinen region appeared to be somewhat cooler, wetter and snowier than the

surrounding areas of inland southern Finland. The weather station at Lammi Pappila, at a distance of about 20 km, agreed with the climatological temperature, precipitation and snow conditions of the Valkea-Kotinen monitoring site without statistically-significant deviations. For wind speed and solar radiation, we employed measurements performed at Jokioinen, at a distance of about 100 km.

Three metrics were used in this paper to depict and interpret the projected (or observed) changes in climate. The first measure refers to the uncertainty in the projections due to inter-model scatter; the second to the statistical significance of the modelled future (or observed past) changes relative to the current climate; and the third to spatially-averaged unforced climate variability in contrast to anthropogenic climate change. Our main interest was on the rate of future climatic changes compared with the variations to which the ecosystems in the Valkea-Kotinen region have been recently exposed. Although we focused on detecting significant trends, it may be noted that even fluctuations and tendencies not exceeding the level of statistical significance may have impacts of practical importance.

The observed increases in annual and spring mean temperature of 0.4 °C, a thinning of the annual mean snow depth by slightly above 1 cm, a shortening of the lake-ice season by 17 days and an advance of its end by six days, all given per decade, are already currently statistically significant, and these trends are also likely to continue in the future. For the majority of the climatic variables, the changes experienced so far have been relatively modest compared to recent inter-annual variations. Already during the next three decades, however, increases in winter, summer and autumn temperatures, increases in annual precipitation, decreases in winter mean snow depth and decreases in winter mean incident solar radiation are projected to emerge from the background of observed inter-annual variability. Based on the rates of changes presented by Räisänen and Eklund (2012), decreases in spring and autumn mean snow depth might already be significant at that stage, but at the latest some decades afterwards. Decreases in spring solar radiation and increases in annual and seasonal mean precipitation sums are also projected to be strong enough to surpass the limit of statistical significance by the 2080s. As an exception, the projected changes in summer precipitation are small and unclear in sign. This applies to summer solar radiation as well.

For a few climatic variables, previous statistically-significant trends are levelling out. These include mean wind speed as well as autumn solar radiation. The projected future increases in autumn solar radiation are small in comparison with the past increases during the European-scale "brightening" episode. Instead of the weakening that has occurred at the considered weather station in the past, the wind speed is projected to undergo slight increases.

The future projections considered in this paper are based on the CMIP3 global climate models and the SRES emission scenarios that have been widely utilized in IAV studies. However, the CMIP3 models are currently being replaced by a new generation of global climate models (CMIP5), and the simulations by them are performed assuming the so-called Representative Concentration Pathway (RCP) scenarios (Taylor *et al*. 2012, Meinshausen *et al*. 2011). Accordingly, new climate change scenarios for Finland based on the CMIP5 models are planned to be produced by the authors in the near future and will become available for use in IAV studies.

Tailored climate change information, often required for vulnerability assessment of ecosystem services, should be offered in a form that affords ready applications. Further studies are needed about small-scale climate phenomena and regional variations in climate because they are particularly relevant for local and regional planning and decision-making. As underlined by Deser *et al*. (2012), it is also essential to more effectively communicate the role of natural climate variability in limiting the accuracy of regional climate predictions. Our study on climate in the Valkea-Kotinen region attempts to serve as a step towards these goals.

Acknowledgements: This work was partially funded by the LIFE+ instrument of the EU via VACCIA (project LIFE07 ENV/FIN/141); the SETUILMU research activity of the Advisory Board for Sectoral Research via the SETUKLIM project; the Academy of Finland through the ClimNext (no. 127239), ADAPT (no. 260785) and FICCA/RECAST (no. 140797) projects. The climate model data were downloaded

from WCRP CMIP3 Multi-Model data archive, supported by the Program for Climate Model Diagnosis and Intercomparison (PCMDI) and the WCRP's Working Group on Coupled Modelling (WGCM). The weather observations were downloaded from the climate data archive of the Finnish Meteorological Institute. The ice-on and ice-off data is based on the observations carried out during several projects funded by the Academy of Finland (METHANO, PRO-DOC), EU (CLIMFRESH, REFLECT, CLIME, EURO-LIMPCS) and other funding organisations. The Finnish Game and Fisheries Research Institute and Lammi Biological Station are also gratefully acknowledged for their support for the lake ice data collection. We are grateful to Dr. Jouni Räisänen for providing additional climate model results, to Pirkko Karlsson for technical aid, to the large number of volunteers who have performed snow measurements in Finland on 15 March every year since 1919, and to contributors to the R Project for Statistical Computing.

References

Aalto J., Pirinen P., Heikkinen J. & Venäläinen A. 2013. Spatial interpolation of monthly climate data for Finland: comparing the performance of kriging and generalized additive models. *Theor. Appl. Climatol.* 112: 99–111.

Ahti T., Hämet-Ahti L. & Jalas J. 1968: Vegetation zones and their sections in northwestern Europe. *Ann. Bot. Fennici* 5: 169–211.

Brockwell P.J. & Davis R.A. 2002. *Introduction to time series and forecasting*, 2 ed. Springer-Verlag, New York.

Coles S. 2001. *An introduction to statistical modeling of extreme values*. Springer-Verlag, London.

Coumou D., Robinson A. & Rahmstorf S. 2013. Global increase in record-breaking monthly-mean temperatures. *Clim. Change*. 118: 771–782.

Critchfield H.J. 1966. *General climatology*, 2nd ed. Prentice Hall, Englewood Cliffs, N.J.

Deser C., Knutti R., Solomon S. & Phillips A.S. 2012. Communication of the role of natural variability in future North American climate. *Nature Climate Change* 2: 775–779.

Forsius M., Anttila S., Arvola L. Bergström I., Hakola H., Heikkinen H.I., Helenius J., Hyvärinen M., Jylhä K., Karjalainen J., Keskinen T., Laine K., Nikinmaa E., Peltonen-Sainio P., Rankinen K., Reinikainen M., Setälä H. & Vuorenmaa J. 2013. Impacts and adaptation options of climate change on ecosystem services in Finland: a model based study. *Current Opinion in Environmental Sustainability* 5: 26–40.

Graham L.P., Hagemann S., Jaun S. & Beniston M. 2007. On interpreting hydrological change from regional climate models. *Clim. Change* 81: 97–122.

Gregow H., Peltola H., Laapas M., Saku S. & Venäläinen A. 2011. Combined occurrence of wind, snow loading and soil frost with implications for risks to forestry in Finland under the current and changing climatic conditions. *Silva Fennica* 45: 35–54.

Gregow H., Ruosteenoja K., Pimenoff N. & Jylhä K. 2012. Changes in the mean and extreme geostrophic wind speeds in northern Europe until 2100 based on nine global climate models. *Int. J. Climatol.* 32: 1834–1846.

Hannula H.-R. 2012. *Napapiirin eteläpuolisen Suomen lumipeite maaliskuussa 1919–2010*. M.Sc. thesis, Department of Geography and Geology, University of Turku.

Harvey B.J., Shaffrey L.C., Woollings T.J., Zappa G. & Hodges K.I. 2012. How large are projected 21st century storm track changes? *Geophys. Res. Lett.* 39, L18707, doi:10.1029/2012GL052873.

Haylock M.R., Hofstra N., Klein Tank A.M.G., Klok E.J., Jones P.D. & New M. 2008: A European daily high-resolution gridded dataset of surface temperature and precipitation. *J. Geophys. Res.* 113, D20119, doi:10.1029/2008JD10201.

Heikinheimo M., Venäläinen A. & Tourula T. 1996. Microclimatic models estimation of components of the energy balance over land surfaces. In: Roos J. (ed.), *The Finnish research programme on climate change*, Final report, Publications of the Academy of Finland 4/96, pp. 62–67.

Helsel D.R. & Hirsch R.M. 2002. *Statistical methods in water resources*, Techniques of Water-Resources Investigations of the United States Geological Survey, Book 4, Hydrologic Analysis and Interpretation, Chapter A3, U.S. Geological Survey.

Hirsch R.M., Slack J.R. & Smith R.A. 1982. Techniques of trend analysis for monthly water quality data. *Water Resources Research* 18: 107–121.

*Holmberg M., Futter M.N., Kotamäki N., Fronzek S., Forsius M., Kiuru P., Pirttioja N., Rasmus K., Starr M. & Vuorenmaa J. 2014. Effects of a changing climate on the hydrology of a boreal catchment and lake DOC — probabilistic assessment of a dynamic model chain. *Boreal Env. Res.* 19 (suppl. A): 66–82.

Hällfors M.H., Lindén L., Rita H. & Schulman L.E. 2011. Using a botanic garden collection to test a bioclimatic hypothesis. *Biodiversity and Conservation* 20: 259–275.

IPCC 2007. *Climate change 2007. The physical science basis*. Contribution of Working Group I to the Fourth Assessment Report of the Intergovernmental Panel on Climate Change. Cambridge University Press, Cambridge, United Kingdom and New York, NY, USA.

Jokela A. 2011. *Sään ääri-ilmiöt luonnollista vaihtelua kuvaavassa 1200-vuotisessa ilmastokokeessa*. M.Sc. thesis, Department of Physics, University of Helsinki.

Jylhä K., Fronzek S., Tuomenvirta H., Carter T.R. & Ruosteenoja K. 2008. Changes in frost, snow and Baltic Sea ice by the end of the twenty-first century based on climate model projections for Europe. *Clim. Change* 86: 441–462.

Jylhä K., Tuomenvirta H., Ruosteenoja K., Niemi-Hugaerts H., Keisu K. & Karhu J.A. 2010. Observed and projected future shifts of climatic zones in Europe, and their use to visualize climate change information. *Weather, Climate, and Society* 2: 148–167.

Jylhä K., Ruosteenoja K., Räisänen J., Venäläinen A., Tuomenvirta H., Ruokolainen L., Saku S. & Seitola T. 2009. *Arvioita Suomen muuttuvasta ilmastosta sopeutumis-tutkimuksia varten. ACCLIM-hankkeen raportti 2009* [*The changing climate in Finland: estimates for adaptation*

studies. ACCLIM project report 2009]. Reports 2009:4, Finnish Meteorological Institute, Helsinki. [In Finnish, abstract, extended abstract, figure captions and tables also in English].

Jönsson A.-M. & Bärring L. 2010. Future climate impact on spruce bark beetle life-cycle in relation to uncertainties in regional climate model data ensembles. *Tellus* 63A: 158–173.

Kersalo J. & Pirinen P. 2009. *Suomen maakuntien ilmasto* [*The climate of Finnish regions*]. Reports 2009: 8, Finnish Meteorological Institute, Helsinki. [In Finnish with English summary].

Köppen W. 1936: Das geographische System der Klimate. In: Köppen G. (ed.), *Handbuch der Klimatologie*, vol. I, Part C, Gebrüder Borntraeger, Berlin, pp. C1–C4.

Laapas M., Jylhä K. & Tuomenvirta H. 2012. Climate change and future overwintering conditions of woody, horticultural plants in Finland. *Boreal Env. Res.* 17: 31–45.

Marchetto A., Rogora M. & Arisci S. 2013. Trend analysis of atmospheric deposition data: a comparison of statistical approaches. *Atmospheric Environment* 64: 95–102.

Meehl G.A., Covey C., Delworth T., Latif M., McAvaney B., Mitchell J.F.B., Stouffer R.J. & Taylor K.E. 2007. The WCRP CMIP3 multimodel dataset: a new era in climate change research. *Bull. Amer. Meteor. Soc.* 88: 1383–1394.

Meinshausen M., Smith S.J., Calvin K., Daniel J.S., Kainuma M.L.T., Lamarque J.-F., Matsumoto K., Montzka S.A., Raper S.C.B., Riahi K., Thomson A., Velders G.J.M. & van Vuuren D.P.P. 2011. The RCP greenhouse gas concentrations and their extensions from 1765 to 2300. *Clim. Change* 109: 213–241.

Myllys H. 1999. *Alli-myrsky ja Hirlamin tuuliennusteet*. M.Sc. thesis, Department of Meteorology, University of Helsinki.

Morak S., Hegerl G.C. & Christidis N. 2013. Detectable changes in the frequency of temperature extremes. *J. Climate* 26: 1561–1574.

Nakićenović N. & Swart R. (eds.) 2000. *Special Report on Emissions Scenari*os. A Special Report of Working Group III of the Intergovernmental Panel on Climate Change. Cambridge University Press, Cambridge, United Kingdom and New York, NY, USA.

Nikulin G., Kjellstrom E., Hansson U., Strandberg G. & Ullerstig A. 2011. Evaluation and future projections of temperature, precipitation and wind extremes over Europe in an ensemble of regional climate simulations. *Tellus* 63A: 41–55.

Orlowsky B. & Seneviratne S.I. 2012. Global changes in extreme events: regional and seasonal dimension. *Clim. Change* 110: 669–696.

Otto F.E.L., Massey N., van Oldenborgh G.J., Jones R.G. & Allen M.R. 2012. Reconciling two approaches to attribution of the 2010 Russian heat wave. *Geophys. Res. Lett.* 39, L04702, doi:10.1029/2011GL050422.

Peltola H., Ikonen V.-P., Gregow H., Strandman H., Kilpeläinen A., Venäläinen A. & Kellomäki S. 2010. Impacts of climate change on the forest dynamics and timber production with implications on the regional risks of wind-induced damage to forests in Finland. *Forest Ecology and Management* 260: 833–845.

Pirinen P., Simola H., Aalto J., Kaukoranta J.-P., Karlsson P. & Ruuhela R. 2012. *Tilastoja Suomen ilmastosta 1981–2010* [*Climatological statistics of Finland 1981–2010*]. Reports 2012:1, Finnish Meteorological Institute, Helsinki. [In Finnish and English].

R Core Team 2012. *R: A language and environment for statistical computing*. R Foundation for Statistical Computing, Vienna, Austria. [Available at http://www.R-project.org/].

Rummukainen M. 2010. State-of-the-art with regional climate models. *WIREs Climate Change* 1: 82–96.

Roeckner E., Bäuml G., Bonaventura L., Brokopf R., Esch M., Giorgetta M., Hagemann S., Kirchner I., Kornblueh L., Manzini E., Rhodin A., Schlese U., Schulzweida U. & Tompkins A. 2003. *The atmospheric general circulation model ECHAM5. Part 1: Model description*. MPI Report 349, Max Planck Institute for Meteorology, Hamburg, Germany.

Ruoho-Airola T. 2012. Comparison of atmospheric concentrations of sulphur and nitrogen compounds, chloride and base cations at Ähtäri and Hyytiälä, Finland. *Boreal Env. Res.* 17: 128–138.

*Ruoho-Airola T., Hatakka T., Kyllönen K., Makkonen U. & Porvari P. 2014. Temporal trends in the bulk deposition and atmospheric concentration of acidifying compounds and trace elements in the Finnish Integrated Monitoring catchment Valkea-Kotinen during 1988–2011. *Boreal Env. Res.* 19 (suppl. A): 31–46.

Ruosteenoja K. 1986. The date of break-up of lake ice as a climatic index. *Geophysica* 22: 89–99.

Ruosteenoja K. & Räisänen P. 2013. Seasonal changes in solar radiation and relative humidity in Europe in response to global warming. *J. Climate*. 26: 2467–2481.

Ruosteenoja K., Tuomenvirta H. & Jylhä K. 2007. GCM-based regional temperature and precipitation change estimates for Europe under four SRES scenarios applying a super-ensemble pattern-scaling method. *Clim. Change* 81, Supplement 1: 193–208.

Ruosteenoja K., Räisänen J. & Pirinen P. 2011. Projected changes in thermal seasons and the growing season in Finland. *Int. J. Climatol.* 31: 1473–1487.

Räisänen J. 2008. Warmer climate: less or more snow? *Clim Dyn.* 30: 307–319.

Räisänen J. & Eklund J. 2012. 21st century changes in snow climate in Northern Europe: a high-resolution view from ENSEMBLES regional climate models. *Clim Dyn.* 38: 2575–2591.

Räisänen J. & Räty O. 2013. Projections of daily mean temperature variability in the future: cross-validation tests with ENSEMBLES regional climate simulations. *Clim Dyn.* 41: 1553–1568.

Saku S., Solantie R., Jylhä K., Venäläinen A. & Valta H. 2011. *Äärilämpötilojen alueellinen vaihtelu Suomessa* [*Spatial variations of extreme temperatures in Finland*]. Reports 2011:1, Finnish Meteorological Institute, Helsinki. [In Finnish with English summary]

Solantie R. 1986. The growing zones for fruit trees and woody ornamental plants in Finland — revision of earlier divisions. *Sorbifolia* 17: 201–209. [In Finnish with English summary].

** Published in this issue*

Solantie R. 1988. Modification of the climatic zones for fruit trees and woody ornamental plants in Finland. *Sorbifolia* 19: 124–126. [In Finnish with English summary].

Solantie R. 2000. *Snow depth on January 15th and March 15th in Finland 1919–98 and its implications for soil frost and forest ecology*. Meteorological publications 42, Finnish Meteorological Institute, Helsinki.

Solantie R. 2004. On the application of hardiness zones of fruit trees and woody ornamentals. *Sorbifolia* 35: 147–158. [In Finnish with English summary].

Solantie R. 2005. Productivity of boreal forests in relation to climate and vegetation zones. *Boreal Env. Res* 10: 275–297.

Taylor K.E., Stouffer R.J. & Meehl G.A. 2012. An overview of CMIP5 and the experiment design. *Bull. Amer. Meteor. Soc*. 93: 485–498.

Tietäväinen H., Tuomenvirta H. & Venäläinen A. 2010. Annual and seasonal mean temperatures in Finland during the last 160 years based on gridded temperature data. *Int. J. Climatol*. 30: 2247–2256.

Tietäväinen H., Johansson M., Saku S., Gregow H. & Jylhä K. 2012. Extreme weather, sea level rise and nuclear power plants in the present and future climate in Finland. In: *11th International Probabilistic Safety Assessment and Management Conference and the Annual European Safety and Reliability Conference 2012 (PSAM11 ESREL 2012)*, Curran Associates, Inc., Red Hook, NY, pp. 5487–5496.

Tuomenvirta H. 2004. *Reliable estimation of climatic variations in Finland*. Contributions 43, Finnish Meteorological Institute, Helsinki.

Vajda A., Tuomenvirta H., Jokinen P., Luomaranta A., Makkonen L., Tikanmäki M., Groenemeijer P., Saarikivi P., Michaelides S., Papadakis M., Tymvios F. & Athanasatos S. 2011. *Probabilities of adverse weather affecting transport in Europe: climatology and scenarios up to the 2050s*. Reports 2011:9, Finnish Meteorological Institute, Helsinki.

Venäläinen A., Tuomenvirta H., Pirinen P. & Drebs A. 2005. *A basic climate data set 1961–2000 — description and illustrations*. Reports 2005:5, Finnish Meteorological Institute, Helsinki.

Venäläinen A., Saku S., Kilpeläinen T., Jylhä K., Tuomenvirta H., Vajda A., Ruosteenoja K. & Räisänen J. 2007. *Sään ääri-ilmiöistä Suomessa [Aspects about climate extremes in Finland]*. Reports 2007:4, Finnish Meteorological Institute, Helsinki. [In Finnish with English abstract].

Venäläinen A., Jylhä K., Kilpeläinen T., Saku S., Tuomenvirta H., Vajda A. & Ruosteenoja K. 2009. Recurrence of heavy precipitation, dry spells and deep snow cover in Finland based on observations. *Boreal Env. Res*. 14: 166–172.

Vuorenmaa J., Arvola L. & Rask M. (eds.) 2011. *Long-term environmental change in Häme — Twenty years of environmental research and monitoring at Valkea-Kotinen supersite*. The Finnish Environment 34/2011, Finnish Environment Institute (SYKE), Helsinki. [In Finnish with English summary].

Weyhenmeyer G., Meili M. & Livingstone D. 2004. Nonlinear temperature response of lake ice breakup. *Geophys. Res. Lett*. 31, L07203, doi: 10.1029/2004GL019530.

Wild M. & Schmucki E. 2011. Assessment of global dimming and brightening in 593 IPCC-AR4/CMIP3 models and ERA40. *Clim. Dyn*. 37: 1671–1688.

Wilks D.S. 2006. *Statistical methods in the atmospheric sciences*, 2nd ed. International Geophysics Series, vol 91, Elsevier.

Willems P., Arnbjerg-Nielsen K., Olssonn J. & Nguyen V.T.V. 2012. Climate change impact assessment on urban rainfall extremes and urban drainage: methods and shortcomings. *Atmospheric Research* 103: 106–118.

WMO 2011. *Guide to climatological practices*. WMO 100, World Meteorological Organization, Geneva.

Ylhäisi J. S., Tietäväinen H., Peltonen-Sainio P., Venäläinen A., Eklund J., Räisänen J. & Jylhä K. 2010. Growing season precipitation in Finland under recent and projected climate. *Nat. Hazards Earth Syst. Sci*. 10: 1563–1574.

Appendix 1. Significance of trends (Mann-Kendall (MK) test). Only cases with $p \leq 0.05$ are shown. Note that significant decreases in monthly mean 10-minute wind speeds in March–December in 1959–2010 and diffuse radiation in about every other calendar month in 1980–2009 are not shown. For Z_S *see* Hirsch *et al.* (1982).

Variable (unit)	Station	Years	*n*	Season	Z_S	*p*	Slope (10 yr)$^{-1}$
Temperature (°C)	4	1964–2011	48	Mar–May	3.28	0.0010	0.44
				Jun–Aug	2.12	0.0344	0.22
				Sep–Nov	2.28	0.0229	0.33
				Annual	3.74	0.0002	0.41
				Apr	3.45	0.0006	0.61
				Jul	2.61	0.0090	0.41
				Sep	2.20	0.0281	0.42
		1990–2010	21	Sep	2.02	0.0431	1.14
Number of days < 0°C (days)	4	1964–2011	48	Annual	–2.73	0.0063	–4.6
				Feb	–2.03	0.0426	–0.3
				Apr	–2.67	0.0075	–1.4
		1990–2010	21	Apr	–2.58	0.0098	–3.1
Length of spells < 0°C (days)	4	1964–2011	48	Dec–Feb	–2.21	0.0268	–4.6
				Feb	–2.03	0.0424	–0.7
				Apr	–2.39	0.0167	–0.6
		1990–2010	21	Jan	2.04	0.0411	3.9
				Apr	–1.96	0.0501	–2.0
Length of spells > 0°C (days)	4	1964–2011	48	Mar–May	2.07	0.0381	2.3
				Jan	2.44	0.0147	0.4
				Apr	2.82	0.0047	2.0
		1990–2010	21	Mar–May	2.30	0.0214	10.0
				Annual	2.45	0.0144	13.5
				Apr	2.61	0.0092	7.5
Precipitation (mm)	4	1964–2011	48	Jan	2.20	0.0275	4.5
				Jun	2.80	0.0051	6.6
Snow depth (cm)	4	1964–2011	48	Annual	–2.18	0.0308	–1.1
				Feb	–1.99	0.0465	–4.0
Lake ice–off (days)	1	1990–2010	21		–3.10	0.0020	–5.7
Lake ice season (days)	1	1990–2010	21		–2.63	0.0086	–17.1
10–minute wind speed (m s^{-1})	8	1959–2010	52	Dec–Feb	–2.08	0.0371	–0.1
				Mar–May	–3.76	0.0002	–0.1
				Jun–Aug	–5.00	6e–7	–0.1
				Sep–Nov	–4.18	3e–5	–0.1
				Annual	–5.67	1e–8	–0.1
Max 10–min wind speed (m s^{-1})	8	1959–2010	52	Mar–May	–3.00	0.0027	–0.3
				Jun–Aug	–3.28	0.0010	–0.3
				Mar	–2.86	0.0042	–0.4
				Jun	–2.96	0.0031	–0.3
		1990–2010	21	Mar	–2.02	0.0437	–0.7
Total solar radiation (MJ m^{-2})	8	1980–2009	30	Sep–Nov	2.00	0.0497	20
				Sep	2.00	0.0457	19
Direct solar radiation (MJ m^{-2})	8	1980–2009	30	Mar–May	2.57	0.0102	50
				Sep–Nov	2.64	0.0083	27
				Annual	3.03	0.0024	112
				Sep	2.36	0.0185	22
		1990–2009	21	Mar–May	2.04	0.0410	63
Diffuse solar radiation (MJ m^{-2})	8	1980–2009	30	Dec–Feb	–3.00	0.0027	–6
				Mar–May	–3.82	0.0001	–22
				Jun–Aug	–3.55	0.0004	–32
				Annual	–4.17	3e–5	–70
		1990–2009	21	Annual	–2.11	0.0350	–46
				Jun	–2.11	0.0350	–18

Appendix 2. Significance of differences in temperature at station 4 between the periods 1964–1989 (n = 26) and 1990–2010 (n = 21) [Welch t-test (Wt)]. Only cases with $p < 0.05$ are shown.

Season	df	t	p	Increase
Dec–Feb	45.0	2.84	0.0068	2.4
Mar–May	43.2	2.83	0.0070	0.9
Annual	42.8	4.13	0.0002	1.0
Jan	41.4	2.58	0.0134	3.1
Apr	41.5	3.81	0.0004	1.5
Aug	35.5	2.98	0.0052	1.0

Appendix 3. Significance of differences in selected variables at station 4 between the periods 1964–1989 (n = 26) and 1990–2010 (n = 21) (Mann-Whitney (MW) tests). Only cases with $p < 0.05$ are shown. For Z *see* Wilks (2006: 157–158)

Variable	Season	Z	p	Difference
Number of days < 0 °C	Dec–Feb	–2.42	0.0159	–7.9
	Annual	–2.30	0.0220	–10.9
	Jan	–2.04	0.0403	–2.2
	Feb	–2.24	0.0231	–3.0
	Apr	–2.11	0.0355	–2.9
Length (days) of spells < 0 °C	Dec–Feb	–2.76	0.0059	–18.2
	Annual	–2.34	0.0196	–12.6
	Jan	–2.46	0.0135	–6.7
	Feb	–2.35	0.0174	–5.8
	Apr	–1.99	0.0461	–1.7
Length (days) of spells > 0 °C	Dec–Feb	2.34	0.0393	2.2
	Jan	2.52	0.0233	1.2
	Feb	2.47	0.0240	1.6
	Apr	2.60	0.0214	4.4
Snow depth (cm)	Dec–Feb	–2.18	0.0289	–7.7
	Mar–May	–2.42	0.0151	–6.5
	Annual	–2.57	0.0096	–3.6
	Feb	–2.19	0.0291	–11.4
	Mar	–2.56	0.0109	–12.9
	Dec	–2.03	0.0432	–4.6